The Multiple Roles of Gamma Interferon in Intraepithelial T Cell-Villous Enterocyte Interactions in Active Celiac Disease

Johnson JE[1*], Agrawal K[1*], Al-Lamki RS[1,2], Zhang F[1], Wang Xi[3], Liburd Jr S[3], Tobiasova Z[1], Rodriguez L[4], Martins AJ[1], Sefik E[1], Flavell RA[1], Robert ME[3] and Pober JS[1,3]

1. Department of Immunobiology. Yale School of Medicine
2. Department of Medicine, Addenbrooke's Hospital
3 Department of Pathology, Yale School of Medicine
4. Yale Pediatric Gastroenterology and Hepatology

*These authors contributed equally.

Supported by a Yale School of Medicine Teams Award and grants for the Colton Center for Autoimmunity at Yale to MRE, JSP, ES and RAF. JEJ is supported by the MSTP T32 training grant. RSA-L is supported by National Institute for Health and Care Research Cambridge Biomedical Research Centre at the Cambridge University Hospitals National Health Service Foundation Trust. ES is supported by a grant from the Celiac Disease Foundation.

Abstract

We identified molecular interactions between duodenal enterocytes and intraepithelial T cells in celiac disease (CeD) vs normal controls. We observed an expected increased ratio of T cells [bearing either T cell receptor (TCR) αβ or γδ and mostly activated cytotoxic T lymphocytes (CTLs) expressing granzyme B, CD45RO, Ki67 and Nur 77 proteins as well as IFNγ mRNA] to villous enterocytes. Few T cells (<5%) express NKG2C or DAP12 proteins. CeD villous enterocytes express an IFNγ signature (by single cell RNA sequencing and nuclear phopho-STAT1 and HLA-DR protein staining). CeD enterocytes express increased IFNγ-inducible chemokines CCL3, CCL4, CXCL10 and CXCL11 mRNA while CeD intraepithelial T cells express reduced levels of CCR5 and CXCR3 chemokine receptors, suggesting ligand-induced downregulation. CeD enterocyte HLA-E mRNA and protein are upregulated whereas HLA-B mRNA but not protein increases. Proximity ligation detected frequent interactions of αβ and γδ TCRs with HLA-E and HLA-B but not with HLA-DR and fewer NKG2C interactions with HLA-E. We suggest that CeD IFNγ-producing TCR αβ and γδ CTLs are recruited into villous epithelium by IFNγ-induced enterocyte production of CCR5 and CXCR3-binding chemokines and kill villous enterocytes primarily by TCR engagement with class I HLA molecules, including HLA-E, likely presenting gluten peptides. The IFN-γ signature of CeD villous enterocytes is a potential biomarker of active disease and a therapeutic target.

Introduction

Celiac disease (CeD) is a common immunological disorder estimated to affect at least 1% of the U.S. population. In affected individuals, ingestion of grains (wheat, barley or rye) containing gluten proteins (gliadins or glutenins) triggers an adaptive immune response that causes both gastrointestinal and systemic symptoms[1-3]. The lack of approved therapy other than dietary avoidance of gluten-containing foods highlights the need to identify new mechanisms and insights for treatment[4, 5].

Although almost all individuals with CeD have an inherited HLA-DQ2 or DQ8 allele found at a frequency of 30% in the total population, only about 1 in 30 develop CeD[6, 7]. Certain class I HLA alleles also convey a risk, but this may be from linkage disequilibrium to HLA-DQ2[6]. Mechanistically, the initiating event in developing CeD is activation of naïve CD4 T cells that recognize gluten-derived peptides that have undergone deamidation by tissue transglutaminase (TTG)[8, 9]. Deamidated gluten peptides (DGPs) are presented to DGP-reactive CD4 T cells by antigen presenting cells, likely HLA-DQ2- or DQ8-expressing dendritic cells within gut-draining lymph nodes[10]. The unique ability of these two HLA-DQ alleles to bind and present DGPs explains the HLA association. Once activated DGP-reactive CD4 T cells differentiate into T helper cells that 1). promote B cell antibody responses against gluen peptides or transglutaminase and 2). likely provide help for development of reactive cytotoxic T lymphocytes (CTLs)[3, 11] which may express either $\alpha\beta$ or $\gamma\delta$ T cell receptors for antigen (TCRs). These CTLs may recognize gluten peptides bound to certain class I HLA molecules[12]. In active or established CeD, both CD4 T and B cells home to and accumulate within the lamina propria of

the small bowel[13-15]. Activated CTLs, however, traverse pass the lamina propria to enter the epithelial lining of the small intestinal villi, replacing the normally resident protective intraepithelial T cell populations[16]. Recruited intraepithelial CTLs can cause villous enterocyte dysfunction and death, but the activating signals displayed on the enterocytes are unclear. Loss of villous enterocytes produces the villous flattening characteristic of active CeD and results in malabsorption, the underlying cause of many CeD symptoms[15, 17, 18].

CTL recruitment to the villous epithelium is likely driven by chemokines. The homeostatic chemokine CCL25 is constitutively produced by the small intestine and contributes to homing of CTLs, CD4 T cells, and other cell types to the intestinal lamina propria, but it is unclear if CCL25 further drives CTLs into the epithelium[19, 20]. In other settings CTL recruitment is driven by inflammatory rather than tissue-specific chemokines, particularly those that bind to chemokine receptor CCR5 (e.g., CCL3, 4 and 5) and/or to CXCR3 (e.g., CXCL-9, 10, and 11)[19]. Prior studies have proposed a role of CXCR3 ligands in CTL recruitment to the gut as they are increased in CeD, but less is known about which ones drive specific recruitment to the epithelium[21, 22]. A recent study has provided similar evidence for CCR5 ligands in driving CTL recruitment[23].

CTLs kill target cells either by granule exocytosis leading to release of cytotoxic molecules like perforin, granzyme B and granulysin or by surface expression of molecules such as Fas ligand that engage “death receptors” on the target cell [24]. Both pathways of CTL killing are contact-dependent, requiring recognition of a ligand on the target cell that engages an activating receptor on the CTL to trigger exocytosis of death-inducing effector molecules[25].

Conventionally, the activating receptor on CTLs is the TCR, which upon binding to a specific (typically microbe-derived) peptide/class I MHC molecule complex, will induce granule exocytosis through signaling initiated by the TCR-associated CD3 protein complex [24]. Conventional class I MHC molecules are encoded by the most polymorphic genes in the genome with over a thousand different alleles in the human population, although any individual expresses only 6 alleles, two at each class I (HLA-A, -B or -C) locus[26]. These polymorphic variations in protein sequence determine which peptides are able to bin to the HLA molecule. The T cell population in each individual will also clonally express trillions of different TCRs. This diverse TCR repertoire arises from somatic rearrangements of the genes encoding the two TCR protein chains during thymic development where selection takes place, resulting in clonally expressed TCRs that specifically recognize epitopes formed from both polymorphic amino residues of the inherited self HLA molecules and amino acid residues of the bound non-self-derived peptides[27]. Consistent with this mechanism of antigen recognition, CTLs in the blood or in the epithelial lining of the duodenum in CeD patients following a gluten dietary challenge have been shown to react to gluten-derived non-self-peptides presented by various HLA-A or B proteins[28]. Furthermore, since specific class I HLA alleles are often in linkage disequilibrium with HLA-DQ2, it is likely that a class I allele capable of binding gluten peptides will be found in an HLA-DQ susceptible individual[18, 28, 29]. Importantly, some of the gluten-induced blood and duodenal CTL populations share the same TCRs, implying they are descendants of a common naïve T cell and further suggests that that at least some intraepithelial CTLs arise from homing of the circulating CTLs generated in the secondary lymph nodes[18].

While most peptides presented to CTL involve a conventional class I HLA molecule, a small number of peptides associated with a few infectious organisms may also be presented by HLA-E even though this unusual class I molecule has very limited polymorphisms, with only two common alleles in the human population[30]. However, HLA-E can also be recognized by natural killer (NK) cells bearing an inhibitory receptor (NKG2A) or an activating receptor (NKG2C). Highly activated CTL may also express NKG2C and kill target cells displaying HLA-E, bypassing a role for antigen recognition by a TCR[31]. In CeD, some intraepithelial CTL do express NKG2C and villous enterocytes in CeD strongly express HLA-E, supporting an alternative hypothesis of enterocyte killing, namely that intraepithelial CTL kill villous enterocytes by NKG2C engagement of HLA-E in a manner that is independent of antigenic gluten peptides[31]. Gluten peptides may still play a role in NKG2C-mediated killing because they can stabilize HLA-E, significantly increasing its expression on the cell surface. Activating signals from HLA-E-engaged NKG2C are initiated by an adaptor molecule called DAP12 instead of through the TCR-associated CD3 complex of proteins.

Here we present findings that address some unanswered questions in CeD. Our data suggest that intraepithelial CTL-derived IFN-γ acts on villous enterocytes to induce both inflammatory chemokine production and increased expression of MHC molecular targets, especially HLA-E, for CTL-mediated killing. Downregulation of relevant chemokine receptors on intraepithelial T cells in CeD suggests that a response to some of these inflammatory chemokines has occurred and could account for recruitment of CTL into the epithelial layer. We further show by proximity ligation assays that CTL-mediated killing of enterocytes likely occurs

primarily through TCR:Class I HLA interactions, including both conventional and non-conventional HLA-E, rather than by NKG2C recognition of HLA-E.

Methods

Single cell RNA-sequencing analysis of human duodenal biopsies

Raw sequencing data were processed using CellRanger software (v7.0.1) and aligned to the reference genome GRCh38-2020-A. Filtered output from CellRanger was used for downstream processing using R (v4.3.3) and Seurat (v5.0.0). The analysis pipeline consisted of filtering cells based on mitochondrial gene counts less than 50%, which is consistent with other single cell RNA-sequencing studies of small intestinal tissue[32]. Gene expression was normalized and log-transformed. Cells identified as doublets by scDblFinder (v1.16.0) were removed[33]. Harmony (v1.2.0)[34] was used to compute a batch-corrected embedding of the samples and to integrate the individual patient data. After integrating the data, Celltypist (v.1.3.0)[35] and the human gut reference[32] included by Celltypist were used to annotate cells. Annotations were then manually confirmed using known marker genes and labeled a population of cycling T cells (MKI67+, TOP2A+, CD3D+) cells not identified by celltypist. Finally, a Wilcoxon Rank Sum Test was used to find differentially expressed genes between the celiac and control samples for each cell type individually.

Tissue processing and single cell droplet encapsulation

Duodenal mucosal biopsies for research were obtained with informed consent from 3 patients with CeD (with moderate villous flattening (Marsh grade 3A) and 3 patients with normal mucosa undergoing diagnostic endoscopy. All six samples were deidentified prior to transfer to the laboratory under a protocol approved by the Yale Institutional Review Board. Research biopsies were immediately immersed in RPMI containing 1 mM DTT, 20 mM EDTA and 2% FBS at 37° C for 15 min to isolate epithelial cells and dissociated in Liberase TL (200 μg/ml of

Liberase TL) containing solution in RPMI for 20 min at 37°C. Digested cell suspensions were passed through a 100-μm cell strainer at least three times, washed with complete media, and combined with the epithelial fraction before processing for droplet-based single-cell RNA-seq (scRNA-seq). To ensure 10,000 cells were encapsulated into droplets using 10x Chromium GEM technology single cells were suspended at 1,500 cells/ microliter concentration. Libraries were prepared in house using the Chromium Next GEM Single Cell 3' Reagent Kits v.3.1 (10x Genomics). scRNA-seq libraries were sequenced using the Nova-Seq system.

Immunofluorescence analysis of duodenal mucosa

All human tissue samples used in these studies were de-identified and declared as not human subjects research by the Yale Institutional Review Board. Formalin fixed paraffin embedded (FFPE) duodenal mucosal diagnostic biopsies were obtained from CeD positive cases and/or from patients in whom CeD and other pathological changes were ruled out (normal controls), all accessed through the Yale Department of Pathology. Because the degree of morphological severity can vary at different sites within the duodenum of the same CeD patient, common diagnostic practice is to take multiple duodenal mucosal biopsies during a single endoscopy. The Marsh-Oberhuber Score is used as an index to classify different stages of tissue injury in celiac disease with score 3C being the most severe, showing complete villous blunting, crypt hyperplasia, and increased ratios of intraepithelial T cells to enterocytes[36]. For analysis of FFPE CeD biopsies in this study, we selected biopsy specimens with a Marsh-Oberhuber Score of 3B-3C. The sex and age of the patient and control samples analyzed are summarized in Supplementary Table 1. For each parameter assessed, archival FFPE biopsies

from CeD patients and normal controls (i.e. no pathological changes identified) were screened by a pathologisit (MER) to identify relevant tissue fragements and then re-embedded as individual samples or as multiple (5-6 μm) CeD and control samples from different patients displayed on a single slide as a tissue microarray (TMA) (Supplemetary Table 2). For analysis, the data from multiple samples are pooled for each parameter examined and the numbers of different biopsies analyzed for that parameter are noted in the legend of each figure. One TMA was also created using paired biopsies from five CeD patients who had tissue sampled at the time of diagnosis and later after symptom abatement on a gluten free diet.

For IF staining, tissues were deparaffinized by graded washes in xylene and ethanol. Antigen retrieval was then performed using citrate-based antigen unmasking solution (Vector, H-3300) with samples either heated to 95°C in solution on a hot plate for 30 minutes or using pressure cooker for 5 minutes. Sections were incubated with blocking buffer (1% BSA, 5% donkey or serum in PBS) for 1hr at room temperature (RT) to block nonspecific binding of antibodies to tissue. Primary antibodies were then added overnight at 4°C (Supplementary Table 3), then incubated with appropriate AlexaFluor-conjugated secondary antibodies in blocking buffer (1:200) for 1hr at RT. All antibodies used were validated by the vendor and by using tonsil, spleen, and/or Crohn's disease tissue to confirm reactivity and specificity. Secondary only and isotype controls were used to distinguish signal from background fluorescence.

Cyclic Immunofluorescence (CycIF) of FFPE tissue

CycIF involves repeated staining and imaging of the same tissue section by quenching the fluorescent signal and adding directly conjugated antibody[37]. Briefly, after tissue staining

coverslips are placed on slides using 10% glycerol in PBS. Once images have been acquired, coverslips are removed by placing slides in PBS for 30 min, then the sections are bleached with 3% H_2O_2 and 20mM NaOH in PBS for 1 hr while exposed to light to quench fluorescence. After thorough washes in PBS, specimens are then restained with conjugated antibodies overnight. Images are recorded at each step and then brought into spatial alignment for colocalization of staining patterns using ImageJ and fluorescence intensity quantified by QuPath[37].

Combined IF and fluorescence in situ hybridization by RNAscope

Fluorescence In situ hybridization was performed on FFPE TMAs comprised of paired diagnostic and follow up duodenal biopsies from CeD patients using RNAScope[38]. In addition, 5 follow up biopsies were obtained while patients were following a gluten-free diet (GFD) and showed reversion to normal or near normal histology. We used RNAscope Multiplex Fluorescent Assay with probes (Advanced Cell Diagnostics -ACD) against Epithelial Cell Adhesion Molecule (EpCAM) (#3120388), IFNG (#310508), CD3 (#426621), Granzyme B (#445978), TCR α chain (#433658), TCR γ chain (#472438), CCL3 (#455331), CCL4 (#455341), CCL25 (#474381), CXCL9 (#440161), CXCL10 (#311851), and CXCL11 (#312701). Assays were either performed at ACD with images visualized using SlideView software or performed in our laboratory following the manufacturer's protocol[38]. Briefly, following dewaxing and dehydration, sections were incubated with H_2O_2 and then target retrieval solution. Protease plus was applied to the sections and C1, C2 and C3 probes prepared and subsequently used to hybridize to the target RNA molecules on slides. Signal amplifiers, AMP1, AMP2 and AMP3 were further added and developed using HRP-C1, -C2 and -C3 in combination with appropriate TSA Vivid dyes,

fluorophore 520, fluorophore 570 and fluorophore 650. Sections were then incubated with primary antibodies to CD3, EpCAM and Apolipoprotein A-IV (ApoA4) followed by fluorescence-conjugated secondary antibodies as described above. Following thorough washes in PBS, sections were visualized on the Stellaris 5 confocal microscope (Leica Microsystems Inc, Deerfield, IL 60015, United States). The total number of positive punctate dots representing RNA transcripts was counted in ten fields of view at 40x magnification on CD3+ cells and EpCAM+ enterocytes within ApoA4+ villous epithelium using ImageJ software version 1.53k. Negative control probe-processed sections were used as background signal and the average/mean quantified.

Combined IF and In Situ Proximity Ligation Assay (PLA)

A NaveniFlex™ Tissue MR (Red/Atto647) PLA kit from Navinci Diagnostics (Uppsala, Sweden) was used following the manufacturer's instructions. Briefly, following dewaxing and hydration, sections were incubated with a combination of two primary antibodies, either against a 1). TCR molecule ($\alpha\beta$ or $\gamma\delta$) and MHC ligand (HLA-E, HLA-B or HLA-DR) or 2). NKG2C and HLA-E overnight at 4°C . Navenibody M1 and R2 probes were then added for 60 min at 37°C, followed by two enzymatic reactions to create a rolling circle amplification. At the post-block stage, primary antibodies to CD3 and Collagen IV (to mark basement membrane of the villous epithelium) were added for 30 minutes, followed by incubation with the detection reagent (Atto647) and fluorescence-conjugated secondary antibodies for 60 min at 37°C. After mounting with Prolong Gold Antifade mountant (P36930, Thermo Fischer) and counterstaining the nuclei with DAPI, PLA red fluorescence spots in villous epithelium, indicative for protein-

protein interaction, were evaluated using confocal microscope. The average percentage of PLA spots in villous epithelium in ten fields of view at 40x Magnification was counted in ImageJ and quantified using GraphPad Prism. For negative controls, the primary antibody was replaced with isotype-specific serum and IF staining with the antibodies of the PLA pair were included in parallel with the PLA as a control to demonstrate effective binding by the primary antibodies in each experiment.

Duodenal Mucosal Organ culture

Normal duodenal mucosa was provided by the Yale Department of Pathology from excised, de-identified and discarded surgical intestinal tissue from patients undergoing Whipple procedures at Yale New Haven Hospital. The serosal side was marked with dye, then put in RPMI on ice until it could be picked up for immediate processing. Subsequently, tissue was cut into small fragments and placed on a foam pad for adhesion. Samples were then cultured at 95% O_2 in a 24-well plate submerged with DMEM supplemented with 10% fetal bovine serum, 2 mM L-glutamine, and penicillin/ streptomycin[39]. Samples were either left unstimulated or were activated by adding 500ng/mL of recombinant human IFNγ (PeproTech 300-02) for 24 hours, followed by fixation in 10% NBF for 24 hours and paraffin embedding.

Image Quantification and Statistics

Whole biopsy images were analyzed by tiling 20x images together using the EVOS Fl Auto 2 microscope or Stellaris confocal microscope. Regions of the villous and crypt epithelium were then selected out based on ApoA4 and Ki67 stain, respectively. Quantification of antigens

expressed on each part of the epithelium was performed using QuPath or ImageJ by calculating the mean fluorescence intensity per epithelial area and for RNAscope and PLA, the total number of spot/dots were counted in villous epithelium in ten fields of view at 40x magnification and results expressed either as average/mean of total number of RNA transcripts or as a percentage of PLA spots. $CD3^+$ T cells were quantified either by measuring mean fluorescence intensity of antigen per CD3 cell or as a percentage of cells with bright or dim/absent staining.

Data are expressed as mean ± SEM. Statistical analyses were performed using GraphPad Prism software. The Mann-Whitney U test was used to make statistical comparisons between two unpaired groups while the Wilcoxon test was used for paired groups. A *P* value of less than or equal to 0.05 was considered statistically significant.

Results

Transcriptional landscape of CeD at single cell level

We began our analyis of CeD using single cell RNA seq to gain a non-biased view of the transcriptional lansdcape of the duodenal mucosa. We analyzed fresh research biopsies from patients whose diagnostic biopsies, taken during the same endoscopy procedure, confirmed active CeD (Marsh Grade 3A) as well as three fresh research biopsies with no specific patholgical changes identified to serve as healthy controls. Single cell RNA sequencing analysis captured every major intestinal mucosal cell type including all subsets of immune cells, epithelial cells and stromal cells (Figure 1A)[32]. Among these, enterocytes and activated T cells exhibited the most significant differences in CeD biopsies from controls. We were not able to cleanly separate T cells from the epithelial layer and the lamina propria even though our procedure for making single cell suspensions involved enrichment for epithelium as a first step. In the initial UMAP embedding, CD8+ TCR αβ cells and TCR γδ cells could not be separated due to their similar transcriptomes. To address this, we took a closer look at the T cell subsets and increased cluster resolution (Figure 1B, C). Both TCR αβ and TCR γδ T cell subsets in CeD were enriched for markers of T cell activation and cytotoxicity and clustered distinctly compared to their counterparts in control biopsies. Among CD4+ TCR αβ cells, there was a marked reduction in IL-17 expressing T cells and an increase in regulatory T cells (Figure 1D). Interestingly, CD4+ TCR αβ cells expressed very little IFNG (Figure 1E). Activated CD8+ TCR αβ had elevated levels of GZMB, NKG7 and IFNG. Additionally, CD8+TCR αβ and TCR γδ T cells were the major cell types that expressed IFNG and exhibited significant expression of IFNG transcript, a feature that was largely absent in the control biopsies (Figure 1E, F, Supplementary Figure 1). Interestingly,

enteroyctes that express villous defining marker APOA4+ showed elevated levels of IFNGR1 (Fig. 1G, H), suggesting an increased responsiveness to IFNγ produced by CeD T cells.

Characteristic Cellular Composition of Villous/Surface Epithelium in CeD and Control Biopsies

Informed by the scRNAseq data, we applied spatial approaches to focus further on the interactions between T cells and enterocytes within the epithelial lining. To do so, we first applied IF to FFPE diagnostic duodenal biopsies from normal controls and CeD patients with severe villous flattening (Marsh grade 3B and C) archived in the Yale Pathology Department. In various experiements, enterocytes were identified using pan-enterocyte markers E-cadherin (Figure 2A) or EpCAM. The villous epithelial compartment, whose boundaries can be difficult to define in CeD, was distinguished from crypt epithelium by ApoA4 expression and by staining of the transitional zone between villi and crypts with Ki-67 (Fig 2B).[40] In some experiments, we demarcated the epithelium from the lamina propria by identification of the epithelial basement membrane with anti-Collagen IV. In accordance with established diagnostic practice, we quantified the number of T cells per 100 epithelial cell nuclei (identified by staining with DAPI). Diagnostic criteria for villous epithelial lymphocytosis in CeD include a threshold >25 intraepithelial lymphocytes per 100 epithelial cells[41]. Our samples of CeD biopsies have an average of 36.1 $\pm$ 2.18 (SEM) CD3 T cells per 100 villous nuclei, and our normal control biopsies have a mean of 14.5 $\pm$ 2.97 CD3 T cells per 100 villous nuclei (Figure 2C, D). After separating this CD3 population on the surface into TCR $\alpha\beta$ and $\gamma\delta$ cells, we still found both populations to be significantly increased in CeD compared normal controls. Specifically, TCR $\alpha\beta$ T cells were present at 25.5 $\pm$ 2.26 T cells per 100 villous enterocyte nuclei in CeD vs. 8.49 $\pm$ 1.5 cells in

controls (Figure 2E). TCR $\gamma\delta$ T cells were present at 7.6 $\pm$ 2.58 T cells per 100 enterocyte nuclei in CeD vs. 1.1 $\pm$ 0.42 in controls (Figure 2F). Interestingly, while the ratios of T cells to villous enterocytes increased in CeD patient biopsies, the ratios between T cells to crypt enterocytes were not significantly different in CeD and control samples. Crypt TCR $\alpha\beta$ cells were present in CeD at a mean of 6.2 $\pm$ 1.7 cells per 100 crypt nuclei vs. 5.5 $\pm$ 1.4 cells in controls while TCR $\gamma\delta$ cells were present in CeD at 1.8 $\pm$ 0.33 cells per 100 enterocyte nuclei vs. 0.5 $\pm$ 0.21 cells in controls (Figure 2G-J). These findings are consistent with prior reports of T cell numbers in the duodenal mucosa in active CeD[42, 43]. The data also indicate that the ratio of T cells to enterocyte nuclei is much higher in the residual villi than in the crypts of the same patient biopsy. While this comparison of villous to crypt T cells in CeD does not reflect total numbers of infiltrating T cells in the different epithelial regions due to villous flattening and crypt elongation, the ratio of T cells to enterocytes is more mechanistically important because it more accurately reflects the average separation distances and the frequency of possible contact-dependent T cell/enterocyte interactions. In other words, such contacts are more likely within the villous portions of the epithelium.

Characterization of intra-epithelial TCR $\alpha\beta$ and TCR $\gamma\delta$ T cell populations in CeD as CTLs

Although transcriptional analysis clearly suggested accumulation of cytotoxic T cells in CeD, our scRNAseq experiments could not determine whether these cells were localized within the epithelial layer. Using IF, we found that a much greater percentage of intraepithelial T cells in CeD than in controls express CD45RO, indicative of prior exposure to their cognate antigen. Specifically, 54.81 ± 4.76% of IELs in CeD express CD45RO+ compared to 27.54 ± 3.76% in

controls (Supplement Fig. 2A). As mentioned, mature CTL can be distinguished by expression of cytosolic granules containing Granzyme B (GrzB) . Thus, we evaluated GrzB expression on the villous and found 38.8 ± 4.8% cells to be GrzB+ in CeD compared to 7.2 ± 1.8% in controls. Increased Granzyme B expression was also observed in both TCR αβ and γδ subsets: TCR αβ cells in CeD were 32.1 ± 7.6% GrzB+ compared to 13.4 ± 5.5% in controls. TCR γδ cells in CeD were 46.1 ± 9.1% GrzB+ compared to 4.68 ± 3.1% in controls (Supplementary Fig. 2B). CD3 T cells in the crypt of CeD patients also had elevated levels of Granzyme B compared to controls: 34.7 ± 10.2% vs. 12.2 ± 5.3% respectively (Supplementary Fig. 2C).It is worth noting that CTL discharge their granules containing GrzB when activated, so a greater percentage may by expressing GZMB transcript.

Because T cells typically synthesize and immediately secrete their newly synthesized cytokines when activated, it is unreliable to assess cytokine production by immunostaining of protein. However, since cytokine production is generally controlled at the level of transcription, we used fluorescence in situ hybridization by RNAscope to assess production of IFNγ, which we identified to be enriched in T cells in our single cell dataset of CeD. CeD patients do not routinely undergo a second round of biopsies if their symptoms improve on a gluten-free diet (GFD). However, we were able to access several patients who did have a second biopsy to determine if the T cell populations were altered by the change in diet. First, we assessed for changes in IFN-γ production on surface T cells and found a significantly greater percentage of CD3 cells were positive for IFN-γ: 49.1± 2.9% positive in active CeD compared to 22.9 ± 4.3% on GFD biopsies (Supplementary Fig. 3B). Both TCR αβ and γδ CTLs in the villous epithelium also showed a similar trend. In TCR αβ CTLs, 19.08 ± 4.04% of the CD3 T cells were IFNγ+ in CeD

compared to 7.91 ± 2.70% on a GFD. In TCR γδ cells, 15.81 ± 4.70% of the CD3 T cells were IFNγ+ in CeD compared to 5.96 ± 1.4% on a GFD (Supplementary Fig. 3C). Thus these patients who required a second biopsy had not fully quiesced their disease, but did show a partial response to gluten avoidance.

In contrast to intraepithelial T cells, T cells in the crypts did not show a significant difference between IFN-γ transcript between, with 18.4 ± 2.8% crypt CD3 T cells expressing IFN-γ in CeD compared to 12.5 ± 2.5 crypt CD3 T cells in controls (Supplementary Fig. 3D). While it was not the focus of this study, analysis of the lamina propria (LP) of the same biopsy also showed few IFN-γ producing T cells and no difference in IFN-γ transcript expression of this population between CeD and control samples, with 15.51 ± 2.6% LP CD3 T cells expressing IFNγ in CeD compared to 12.16 ± 1.78 LP CD3 T cells in controls (Supplementary Fig. 3D). Furthermore, the actual numbers of CD3 T cells in the crypt and LP that express IFNγ are far fewer than in the epithelial layer, consistent with the conclusion that the primary sources of IFN-γ in the duodenal mucosa in CeD patients are the intraepithelial CTLs (Supplementary Fig. 3E).

The synthesis of IFN-γ, detected by message, not only indicates the potential function of the intraepithelial T cells as CTL, but also suggests that these cells are in an activated state, typically as a result of antigen stimulation. As further signs of T cell activation, we found that a significantly higher percentage of intraepithelial T cells in celiac patients express nuclear Ki-67, indicative of proliferation compared to controls, 36.97 ± 4.5% vs 8.76 ± 2.4%, respectively (Fig. 3E, F). Both TCR αβ and TCR γδ T cell subsets also showed an increase in Ki-67 staining: 36.13 ± 5.08% of TCR αβ cells were Ki-67+ in CeD compared to 4.57 ± 3.46% in controls and 46.10 ±

6.95% of TCR γδ cells were Ki-67+ in CeD compared to 8.21 ± 5.15% in controls (Supplementary Figure 4). These findings by staining are consistent with our single cell dataset in which a cycling population of T cells marked by MKI67 expression were present at higher frequency in CeD patients than controls (Fig. 3I), and the staining approach clearly identifies that such changes in CeD occur within the epithelial layer.

In some instances activated CTL can acquire the expression of the NK cell activating receptor NKG2C. A prior study employing single cells isolated from the epithelial layer of CeD biopsies reported that an average of 16% of T cells expressed this marker[31]. However, we found fewer than 5% of intraepithelial CD3 T cells express NKG2C (Figure 3G, H). Additionally, virtually no intraepithelial T cells in our CeD biopsies express the NKG2C-associated signaling protein DAP12 although staining is readily detectable in various LP cell populations in the same biopsies (Figure 3G, H). These findings are consistent with our single cell transcriptomics dataset that shows reduced number of TYROBP (DAP12) expressing T cells in celiac vs. control groups (Figure 3I).

Evidence of IFNγ signaling in villous enterocytes in CeD

Having shown that in CeD the intraepithelial T cell populations (a). express IFNγ mRNA and are thus likely to be actively synthesizing and secreting IFNγ protein and (b) that due to the increased ratios of T cells to villous enterocytes, enterocytes are more likely to be in proximity to an activated T cell, we proceeded to examine surface enterocyte populations for evidence of IFNγ signaling response. The initial response to this cytokine involves Janus kinase (JAK)-mediated phosphorylation of tyrosine residues in the signal transducing and transcriptional

activator 1 (STAT1) protein followed by phosphorylation and dimerization of STAT1, translocation and then accumulation within the nucleus resulting in gene transcription[44]. Assessing for phosphorylated STAT1 in the nucleus, we found significantly increased levels in the villous epithelium of CeD biopsies, with 59.1 ± 6.5% of enterocyte nuclei pSTAT1+ compared to only 1.4 ± 0.45% in normal controls (Figure 4A, B). Phosphorylated STAT1 is also elevated in crypt enterocytes of CeD compared to controls, 24.2% compared to 2.6%, respectively, but this frequency is much lower frequency than in villous enterocytes. In our paired biopsies from individual CeD patients comparing pre- and post GFD, we also observed a decrease in nuclear pSTAT1 expression from 69.5 ± 16.8% of villous enterocytes in active CeD to 9.8 ± 2.2% on a GFD (Supplementary Fig. 5).

Although nuclear pSTAT1 is the hallmark of IFNγ signaling, it is not absolutely specific for IFNγ activation. However, IFNγ is the only human cytokine known to induce class II HLA molecules, such as HLA-DR, on epithelial cell types such as enterocytes. Strikingly, HLA-DR is also increased on villous enterocytes in CeD, with 14.44 ± 4.3% of villous epithelium in CeD positive for HLA-DR compared to 4.52 ± 1.9% in controls. Although minimally, HLA-DR is also elevatd in the crypt, with 2.40 ± 1.38% of crypt epithelium in CeD positive for HLA-DR compared to 0.10 ± 0.03% in controls (Figure 4C, D). Our scRNAseq analysis of enterocytes in CeD revealed a similar increase in class II HLA trascripts in celiac biopsies (Figure 4E).

To confirm that villous enterocytes are responsive to IFNγ, we also performed organ cultures of normal duodenal mucosa. Addition of IFNγ to organ culture leads to upregulation of pSTAT1 expression in 57.4 ± 11.4% of villous nuclei compared to 2.4 ± 1.0 in unstimulated

controls (Supplementary Fig. 6). Of note, IFNγ treatment did not on its own induce enterocyte death in our organ culture experiments.

Evidence supporting IFN-γ in the recruitment of CTLs into the villous epithelium

Next, we explored the hypothesis that IFNγ responses of surface enterocytes could explain, at least in part, CTL infiltration of the epithelial compartment by increasing secretion of specific chemotactic signals. To do so, we first examined expression of chemokine receptors on T cell subsets in our single cell transcriptomics dataset comparing control and celiac biopsies (Supplemetary Fig. 7A, B). In general, T cells showed low expression of chemokine receptor transcripts in CeD samples. Thus, we focused on those chemokine receptors thought to be involved in intestinal recruitment, namely CXCR3, CCR5 , and CCR9[19] . We did not find changes in transcripts of these chemokine receptors in T cells of CeD patients and controls. In contrast, by IF we found that T cells within the surface epithelium of CeD biopsies express CXCR3 and CCR5 at significantly lower expression in CeD compared to controls; whereas, CCR9 was found at similar levels on intraepithelial T cells in both groups (Figure 5A-F). This trend in chemokine expression was the same in TCR αβ and γδ cells of the villous as well (Supplementary Fig. 7C). Since transcript levels did not differ, reduction in protein expression is best explained as downregulation of chemokine receptors after ligand binding and is potentially indicative of a prior chemotactic response[45].

As in the case of cytokines, chemokines are synthesized and immediately secreted by T cells so we turned again to fluorescence in situ hybridization by RNAscope to probe for mRNA encoding known ligands of these receptors. The average number of mRNA hybridized spots per

field encoding two known ligands for CCR5, namely CCL3 and CCL4, were significantly upregulated in the enterocytes of CeD biopsies compared in to controls. CCL3: 76.83 ± 4.47 mRNA spots per field in CeD vs 21.5 ± 1.0 in controls. CCL4: 76.6 ± 2.87 in CeD vs 41 ± 1.01 controls (Fig. 5G, H). In our single cell RNAseq experiments, transcripts for a third ligand for CCR5, namely CCL5, is only minimally expressed by CeD enterocytes, but it is expressed by the activated T cell populations in both CeD and controls. Additionally, both TCR αβ and TCR γδ T cells expressing IFNγ in CeD have higher levels of CCL5 than in controls (Fig. 5I) Two known ligands for CXCR3, namely CXCL10 and CXCL11 were also upregulated in CeD biopsies. CXCL10: 104.54 ± 8.32 mRNA spots per field in CeD vs 55.83 ± 5.11 in controls. CXCL11: 184.67 ± 16.54 in CeD vs 31.67 ± 0.91 in controls (Figure 5J, K). Interestingly, a third known ligand for CXCR3, namely CXCL9, is expressed at lower levels and is only slightly increased in CeD samples. Finally, CCL25, the ligand for CCR9, is more highly expressed by surface enterocytes in CeD biopsies: 247.44 ± 44.33 mRNA spots per field in CeD vs 41.67 ± 8.6 in controls (Fig. 5L). Qualitatively similar findings for these chemokines are seen by single cell RNAseq analysis of isolated ApoA4 expressing enterocytes, but there appear to be quantitative differences. Specifically, the increase in CCL3 and CCL4 appear more pronounced by scRNAseq approach than the increases in CXCL10 and CXCL11. These quantitative differences between the two techniques may reflect the fact that assays were performed on different specimens or the variability in the sensitivity of specific transcripts to analysis by sequencing vs. hybridization.

To link changes in chemokine expression to the actions of IFNγ, we again used organ cultures of duodenal mucosa from resected small bowel samples. RNAscope revealed a similar pattern to the CeD vs. control biopsies in which IFNγ stimulated surface enterocytes had an

increase average number of RNA transcripts per 40X field in CeD as compared to controls. Specifically, we found similar increases in mRNA transcripts in IFNγ-treated organ cultures vs. untreated tissue as we did for CeD biopsies compared controls for chemokines CCL3, CCL4, CXCL10, CXCL11, and CCL25: CCL3: 37.1 ± 0.2 mRNA transcript spots in CeD vs 15.6 ± 0.1 in controls. CCL4: 32.6 ± 0.2 vs 14.3 ± 0.1. CCL25 36.6 ± 0.4 vs. 16.3 ± 0.2. CXCL10: 41.3 ± 0.2 vs 10.6 ± 0.3. CXCL11: 67.3 ± 0.4 vs. 15.3 ± 0.2.. Like our biopsies, we also still observed little change in CXCL9 as well in organ culture. CXCL9: 40.2 ± 0.3 vs. 31.1 ± 0.7 (Supplementary Fig. 8).

Evidence for IFN-γ in CTL recognition of enterocytes

In a final series of experiments we examined if IFNγ effects on surface enterocytes could play a role in CTL-mediated recognition of molecular targets that lead to cell killing. The primary ligands on target cells that can be engaged by the TCRs of CTLs are cognate peptides bound to class I HLA molecules, most often HLA-A, -B, or -C. However, as we noted in the Introduction, HLA-E can also present peptides to the TCRs of CTLs, but due to the limited polymorphism of this locus, only a limited repertoire of peptides can be presented, and it has not been determined if gluten peptides are among those that can be presented in an HLA-E-dependent manner. We first assessed transcript levels of conventional class I molecule HLA-B and non-conventional class I molecule HLA-E in enterocytes in CeD vs. control biopsies in our scRNAseq dataset. All HLA class I transcripts, including HLA-E transcripts, were significantly elevated in all enterocytes including APOA4+ villous enterocytes (Figure 6A). By IF, we also assessed expression of HLA-B, β_2-microglobulin protein (the invariant light chain of all HLA class I proteins), and HLA-E. (We selectively evaluated HLA-B rather than HLA-A and/or -C because of

availability of a B locus-specific antibody that worked well in FFPE tissue.) Since all enterocytes express these proteins to some degree, rather than reporting these data as percent positive enterocytes, we have quantitifed the data as mean fluorescence intensity (MFI) of the epithelial layer. Intraepithelail T cells may contribute to this number in a small way, but the primary source of expression are the enterocytes. Some CeD specimens showed an increase in HLA-B expression, but overall, the change in protein levels detected by staining did not reach statistical significance with MFI of HLA-B expression on villous enterocytes being 122.8 ± 13.4 in CeD compared to 101.1 ± 12.4 in controls (Figure 6B, C). β_2-microglobulin expression on surface epithelium was also not significantly different with MFI in CeD 72.5 ± 7.1 compared to 80.1 ± 8.8 (Figure 6D, E). In contrast, HLA-E protein expression was significantly increased in both the villous and crypt epithelium of CeD biopsies, with villous enterocytes showing HLA-E MFI of 67.5 ± 5.8 in CeD biopsies vs 45.6 ± 4.6 in controls (Figure 6F) and in crypt enterocytes 78.3 ± 7.5 vs 41.8 ± 2.6, respectively (Supplementary Fig. 9). Our organ culture experiment also supported this finding with increased HLA-E expression compared to HLA-B in IFNγ stimulated duodenal mucosa (Supplementary Fig. 10).

To directly assess if TCRs or NKG2C on CTLs have engaged class I HLA molecules on enterocytes, we employed PLA to detect protein-protein interactions. Because this assay only detects targets interacting that are less <40 nm apart, it can sensitively capture and quantify binding interactions between receptors and ligands expressed by interacting cells[46]. TCR $\alpha\beta$, TCR $\gamma\delta$ and NKG2C expressing T cells all showed contacts with enterocyte MHC-I molecules in CeD biopsies compared to controls, which were essentially negative, but the relative frequencies of such interactions varied signficantly (Figure 7A-E, Table 1). As a control, we also

assessed for interaction between TCR and HLA-DR within the epithelium which were rarely observed. Overall, ~33% of CD3 T cells appeared to use their TCR to interact with HLA-B or HLA-E compared to <5% in controls, and this TCR number likely would be larger if we had been able to perform PLA with HLA-A and HLA-C. Importantly, T cells that used their TCRs to engage enterocyte class I MHC molecules frequently expressed Nur77, indicative of TCR signaling. NKG2C does interact with HLA-E, but consistent with the relatively low frequency of expression of this molecule on the intraepithelial T cell population, the frequency of such interactions is much lower than the frequency of TCR engagement with class I HLA molecules.

Discussion

In this study, we have characterized molecular interactions between intraepithelial T cells and enterocytes in duodenal mucosal biopsies from CeD patients vs. controls using a combination of scRNAseq of isolated cells using fresh research biopsies as well as IF/confocal microscopy and fluorescence in situ hybridization (RNAscope) using FFPE biopsies. We restricted the latter spatial analyses to FFPE diagnostic biopsies showing significant morphological change (Marsh-Oberhuber grade 3B-C). In a limited number of cases, we also had follow up biopsies that showed histological resolution**.** Consistent with the literature, we saw increased ratios of intraepithelial T cells to enterocytes and most T cells expressed granzyme B and CD45RO, identifying these cells as CTLs that have had prior contact with antigen[42, 43]. We assessed the activation status of these CTLs by antibody staining for Nur77 or Ki-67 proteins and performed FISH for IFN-γ mRNA and found evidence for a markedly higher frequency of activated CTL in CeD than controls. Interestingly, a higher percentage of the γδ TCR+ CTL expressed GrzB and proliferation marker Ki-67 while a higher percentage of the αβ

TCR+ CTL contained mRNA for IFN-γ[22, 47], but some of both T cell types displayed these markers and it is unclear if these populations have distinct functions. The single cell RNAseq also did not reveal significant differences. Although our current focus is on the epithelial compartment, the lamina propria was also stained in the same biopsies and showed no increase in IFN-γ vs. controls and overall, contained many fewer T cells that produce this cytokine. These data confirm a prior report that intraepithelial CTLs appear to be the only major sources of IFN-γ[48]. The paucity of IFN-γ production by the CD4 T cell populations in the lamina propria is consistent with the identification of these cells as T peripheral helper cells rather than T helper 1 cells[29].

Villous enterocytes in CeD show a classical response to IFN-γ signaling. Specifically, we observed increased levels of nuclear pSTAT1, the principal proximal transcription factor activated by IFN-γ, in CeD tissue that was not observed in duodenal enterocytes in normal biopsies. CeD enterocytes also upregulate HLA-DR, for which IFNγ is the sole known inducer in human resident tissue cells. Our limited analysis of paired biopsies showed that upon starting a GFD, there is a decrease both in IFNγ transcript in intraepthelial T cells and in pSTAT1 expression in enterocytes, but these values did not return to control levels in patients requiring a second biopsy. Since restoration of villous architecture is a slow process, our data suggest the possibility that these responses may be used to monitor CeD activity in clinical trials, although this conclusion needs to be validated in larger studies.

It has been reported that upon gluten challenge in CeD, there is a rapid increase in the level of gluten-reactive CD4 T cells, CD8 αβ T cells and γδ T cells in the circulation followed by a rise of intraepithelial CTLs with overlapping TCRs in the duodenal wall[12]. We suspect T cells in both locations arise primarily from activation of memory T cells in the lymph nodes that drain

the small bowel, but such tissues are not available for analyses to confirm this hypothesis. Upon activation, memory cells rapidly give rise to effector T cells and we expect that effector cells generated within the lymph nodes will first enter the circulation and then home to the small intestinal mucosa. However, while CD4 T cells appear to stop in the lamina propria, CTL bearing $\alpha\beta$ or $\gamma\delta$ TCRs further home to the epithelial layer[18, 29]. We hypothesize that CTLs which arrive to the duodenum, likely in response to the chemokine CCL25 binding to T cell CCR9, must then follow additional chemokines generated with the epithelial layer to induce migration from the lamina propria to the villous epithelium where they cause injury. Immunostaining of CTL within the epithelium of CeD patients compared to controls show reduced levels of CXCR3 and CCR5 protein but not mRNA, with no significant differences in CCR9 levels. These findings are consistent with the downregulation of receptors for inflammatory chemokines due to stimulation by ligand [45]. This interpretation is supported by significantly increased expression of chemokines CCL3 and CCL4 (ligands for CCR5), CXCL10 and CXCL11 (ligands for CXCR3), and CCL25 (ligand for CCR9) in villous enterocytes. In particular, mRNA coding for CXCL10 and CXCL11 were increased in the villous epithelium in CeD patients as compared to the crypt or lamina propria, suggesting it provides a specific recruitment signal to the villous epithelial lining. Organ cultures of normal duodenal mucosa confirmed that villous enterocytes respond to exogenous IFNγ by elevated expression of these same chemokines. Also consistent with prior reports, there is a much smaller increase in significant CXCL9 in enterocytes than in the other two CXCR3 ligands. It is unclear why this is as CXCL9 is often induced coordinately with CXCL10 and CXCL11 in many other cell types. Our organ culture experiments also shown that CCL3, CCL4, and CCL25 are upregulated in villous enterocytes by IFNγ. A third ligand for CCR5, namely

CCL5, is produced primarily by activated T cells. We interpret our data to suggest that newly activated CTLs are recruited from the blood to the villous epithelium by CCR5 and CXCR3 ligands. It remains unclear why CD4 helper T cells remain in the lamina propria. It is possible that TCR engagement blocks chemokine responses as we have seen in some of our prior work[49-51].

Once recruited, CTLs commonly recognize target cells by engagement of their TCRs which have been selected in the thymus to recognize a self-class I HLA molecule with a specific bound peptide, the latter typically derived from a microbial protein. In certain settings, CTL can be activated to express NKG2C, enabling them to target cells expressing HLA-E in a manner independent of antigenic peptide. We found that villous enterocytes express HLA-B protein in control tissues and that only a small overall increase was seen in CeD biospies that did not reach statistical significance. Because all enterocytes are likely to express class I HLA molecules, we have analyzed our data as either mean fluorescence intensity of percent of "brightly staining" cells. In these experiments we used a broadly reactive antibody that binds to all or most different HLA-B alleles. We do not have access to similar antibodies for the HLA-A or HLA-C locus, but there is a similar small but statistically insignificant change in overall staining for β_2-microglobulin, the non-polymorphic light chain of all class I and class I-related HLA molecules. Since the non-polymorphic β_2 microglobulin light chain is shared by all class I HLA molecules, we expect that HLA-A and -C proteins were altered in a manner similar to HLA-B. Our single cell data suggests that mRNAs encoding these proteins are strongly induced and regulation likely takes place post-transcriptionally. We should note that some specimens of CeD did show a significant upregulation of cells that stain brightly for HLA-B (not shown), but many specimens

did not. In contrast, we saw a consistent increase in HLA-E protein in the enterocytes of CeD biopsies. This observation corroborates other studies that have similarly found elevated HLA-E levels on villous enterocytes[31]. This observation has been cited to support the hypothesis that HLE-E is recognized by NKG2C, a natural killer (NK) receptor that can be induced on highly activated CTLs. It has been previously reported that approximately 16% of T cells isolated from the epithelium are NKG2C positive and also express DAP12, the adaptor protein used for its signaling[31]. However, our tissue analysis detected an average of fewer than 5% of intraepithelial T cells expressing NKG2C. Moreover, we did not detect expression of DAP12 in intraepithelial CTL, although it is readily detected within cells of the lamina propria. Another report utilizing scRNAseq also failed to see DAP12 expression in CeD intraepithelial T cells.[22] While our own single cell RNAseq experiments, which could not separate intraepithelial and lamina propria T cells, did show some DAP12 expression, the levels did not differ between CeD and control biopsies. We are uncertain whether the lesser expression of NKG2C and DAP12 we see arises from difference in sensitivity of detection by staining of intact biopsies or from our exclusion lamina propia T cells from our spatial analysis.

The mechanism of HLA-E expression on enterocytes warrants further discussion. mRNAs encoding this protein are induced by IFNγ and we do see increased mRNA in our single cell data. However, HLA-E protein is intrinsically unstable in the absence of bound peptide. Its surface expression normally involves binding of self peptides derived from the signal sequences of other HLA class I molecules, but these peptides are either too limited in quantity or relatively ineffective in stabilizing the protein[52], resulting in low cell surface expression. Despite its limited polymorphisms, the HLA-E locus can present peptides from certain infectious agents, including

Mycobacterium tuberculosis, Human Immunodeficiency Virus and influenza to TCRs[30, 53]. These microbial peptides readily replace the self peptides derived from class I signal sequences and efficiently stabilize HLA-E, resulting in a rise in surface expression. Gliadin-derived peptides have been shown to similarly stabilize and increase HLA-E expression in dendritice cells. [54] Loading of peptides from exogenous proteins into HLA class I molecules is known as "cross-presentation" and is a function normally ascribed to dendritic cells. We do not know if enterocytes can cross-present exogenous peptides or whether glutens and their peptides have unique mechanisms in reaching and binding to nascent HLA-E proteins. In the case of influenza, binding and presentation of an immunodominant peptide actually prevents recognition by NKG2C. We do not know if gluten peptides behave the same way. Rather than classify HLA-E as a non-conventional class I HLA molecule or as a "stress induced protein," it may be more accurate to consider HLA-E as a "specialist" HLA class I molecule similar to the BF1 locus in chickens[55]. Like BF1, HLA-E protein is poorly stabilized by self peptides and normally is expressed at lower levels than HLA-A, -B or -C unless it is exposed to a relevant non-self peptide. Our data provide circumstantial evidence that gluten may, along with the pathogens mentioned above, serve to provide an HLA-E restricted signal to TCRs, a conclusion requiring further experimentation.

In our final set of experiments, we used PLA to directly identify the interactions of intraepithelial CTL receptors with enterocyte class I HLA molecules. PLA is typically employed to observe protein-protein interactions within a single cell, as we have previously used this assay before to study intercellular interactions in renal cell carcinoma[56]. The most abundant interactions involved $\alpha\beta$ TCRs with HLA-E followed by interactions with HLA-B. We did not have

reagents to test interactions with HLA-A or -C, but we expect that these class I molecules could also be relevant. Also as expected, there were no significant interactions of CTL TCRs with HLA-DR, a class II MHC molecule association with peptide presentation to CD4 T cells and there was no significant level of TCR interactions with class I HLA molecules in the control biopsies. We did find NKG2C interactions with HLA-E, but consistent with its infrequent expression on T cells, NKG2C interactions were relatively uncommon compared to TCR interaction. The predominant use of class I HLA molecules to present activating signals to TCRs is consistent with much recent data indicating that CTL, like CD4 cells, can respond to gluten-derived peptides[57, 58].

Our work highlights the importance IFNγ may have in promoting villous atrophy in CeD, acting both as a trigger for CTL cell recruitment to the epithelial layer of the small intestine and for enhancing the capacity of villous enterocytes to present peptides associated with class I molecules to these CTL. In patients with established CeD, partial remission on a GFD reduces but does not eliminate the populations of recruited CTL. In this case, re-exposure to small amounts of gluten may simply provide peptides that can reactivate these residual CTL to generate the signals to recruit new CTL. Still, there appears to be a chicken and egg conundrum: if intraepithelial T cells are the source of IFNγ, how do they produce it within the epithelium before they have been recruited to the epithelium? We do not have an answer to this question, but it is also unclear what triggers CeD to develop in only a subset of patients with susceptible HLA-DQ alleles. The question of what initates CeD is unlikely to be answered by analyzing biopsies of symptomatic patients. Nevertheless, the IFNγ response of the enterocytes described here may prove to be a biomarker of CeD activity and represent a therapeutic target for disrupting CeD pathogenesis.

There are some limitations of this study. First, it is possible that CeD is not a single entity but multiple entities that have different endotypes. Our sample size is not large enough to detect this, but our findings so far do not suggest significant differences among the patients studied that correlate with sex or age. Similarly, our sample size of active vs. quiescing CeD is much too small to establish the IFNγ response as a useful biomarker of disease activity that can guide clinical trials. However, It seems likely that signals such as nuclear pSTAT1 will be much more responsive to disease activity than remodeling of villous architecture. Our PLAs do not establish that the molecular interactions we detect result in TCR signaling. However, we do see Nur77 expression in the same T cells, consistent with activation. Finally, because we are limited to the target organ, i.e. the duodenal mucosa, we cannot establish the conjecture that pathogenic CTL are triggered in the draining lymph nodes and then migrate to the duodenal mucosa. This will require the development of animal models that faithfully recapitulate the human disease. Despite these limitations, we believe that this study has provided evidence to revise the testable hypotheses regarding the mechanisms by which intraepithelial CTLs alter villous architecture and function.

References

[1] Lundin KE, Scott H, Hansen T, Paulsen G, Halstensen TS, Fausa O, Thorsby E, Sollid LM: Gliadin-specific, HLA-DQ(alpha 1*0501,beta 1*0201) restricted T cells isolated from the small intestinal mucosa of celiac disease patients. J Exp Med 1993, 178:187-96.
[2] Molberg O, McAdam SN, Korner R, Quarsten H, Kristiansen C, Madsen L, Fugger L, Scott H, Noren O, Roepstorff P, Lundin KE, Sjostrom H, Sollid LM: Tissue transglutaminase selectively modifies gliadin peptides that are recognized by gut-derived T cells in celiac disease. Nat Med 1998, 4:713-7.
[3] Abadie V, Kim SM, Lejeune T, Palanski BA, Ernest JD, Tastet O, Voisine J, Discepolo V, Marietta EV, Hawash MBF, Ciszewski C, Bouziat R, Panigrahi K, Horwath I, Zurenski MA, Lawrence I, Dumaine A, Yotova V, Grenier JC, Murray JA, Khosla C, Barreiro LB, Jabri B: IL-15, gluten and HLA-DQ8 drive tissue destruction in coeliac disease. Nature 2020, 578:600-4.
[4] Leffler DA, Dennis M, Hyett B, Kelly E, Schuppan D, Kelly CP: Etiologies and predictors of diagnosis in nonresponsive celiac disease. Clin Gastroenterol Hepatol 2007, 5:445-50.
[5] Patel N, Leffler DA, Al-Toma A, Mulder CJ, Elli L, Gan G, Patil P, Atsawarungruangkit A, Kuijpers KC, Del Gobbo A, Goldsmith J, Hintze Z, Pacheco MC, Vieth M, Melcher B, Salomao M, Pai R, Hart J, Olivas A, Naini B, Meyerson C, Choi WT, Kakar S, Westerhoff M, Cheng J, Gopal P, Hammer S, Moreno Prats M, Bronner MP, Robert ME: Clinical Data Do Not Reliably Predict Duodenal Histology at Follow-up in Celiac Disease: A 13 Center Correlative Study. Am J Surg Pathol 2024, 48:212-20.
[6] Sollid LM, Thorsby E: HLA susceptibility genes in celiac disease: genetic mapping and role in pathogenesis. Gastroenterology 1993, 105:910-22.
[7] Gnodi E, Meneveri R, Barisani D: Celiac disease: From genetics to epigenetics. World J Gastroenterol 2022, 28:449-63.
[8] Lundin KEA, Scott H, Fausa O, Thorsby E, Sollid LM: T-Cells from the Small-Intestinal Mucosa of a Dr4,Dq7 Dr4,Dq8 Celiac-Disease Patient Preferentially Recognize Gliadin When Presented by Dq8. Human Immunology 1994, 41:285-91.
[9] Halstensen TS, Scott H Fau - Fausa O, Fausa O Fau - Brandtzaeg P, Brandtzaeg P: Gluten stimulation of coeliac mucosa in vitro induces activation (CD25) of lamina propria CD4+ T cells and macrophages but no crypt-cell hyperplasia. Scand J Immunol 1993, 38:581-90.
[10] Beitnes AC, Raki M, Brottveit M, Lundin KE, Jahnsen FL, Sollid LM: Rapid accumulation of CD14+CD11c+ dendritic cells in gut mucosa of celiac disease after in vivo gluten challenge. PLoS One 2012, 7:e33556.
[11] Lindeman I, Zhou C, Eggesbo LM, Miao Z, Polak J, Lundin KEA, Jahnsen J, Qiao SW, Iversen R, Sollid LM: Longevity, clonal relationship, and transcriptional program of celiac disease-specific plasma cells. J Exp Med 2021, 218:e20200852.
[12] Han A, Newell EW, Glanville J, Fernandez-Becker N, Khosla C, Chien YH, Davis MM: Dietary gluten triggers concomitant activation of CD4+ and CD8+ alphabeta T cells and gammadelta T cells in celiac disease. Proc Natl Acad Sci U S A 2013, 110:13073-8.
[13] Iversen R, Sollid LM: The Immunobiology and Pathogenesis of Celiac Disease. Annu Rev Pathol 2023, 18:47-70.
[14] Jabri B, Sollid LM: Tissue-mediated control of immunopathology in coeliac disease. Nat Rev Immunol 2009, 9:858-70.

[15] Jabri B, Sollid LM: T Cells in Celiac Disease. J Immunol 2017, 198:3005-14.
[16] Oberhuber G, Vogelsang H Fau - Stolte M, Stolte M Fau - Muthenthaler S, Muthenthaler S Fau - Kummer JA, Kummer Ja Fau - Radaszkiewicz T, Radaszkiewicz T: Evidence that intestinal intraepithelial lymphocytes are activated cytotoxic T cells in celiac disease but not in giardiasis. Am J Pathol 1996, 148.
[17] Mayassi T, Ladell K, Gudjonson H, McLaren JE, Shaw DG, Tran MT, Rokicka JJ, Lawrence I, Grenier JC, van Unen V, Ciszewski C, Dimaano M, Sayegh HE, Kumar V, Wijmenga C, Green PHR, Gokhale R, Jericho H, Semrad CE, Guandalini S, Dinner AR, Kupfer SS, Reid HH, Barreiro LB, Rossjohn J, Price DA, Jabri B: Chronic Inflammation Permanently Reshapes Tissue-Resident Immunity in Celiac Disease. Cell 2019, 176:967-81 e19.
[18] Risnes LF, Eggesbo LM, Zuhlke S, Dahal-Koirala S, Neumann RS, Lundin KEA, Christophersen A, Sollid LM: Circulating CD103(+) gammadelta and CD8(+) T cells are clonally shared with tissue-resident intraepithelial lymphocytes in celiac disease. Mucosal Immunol 2021, 14:842-51.
[19] Trivedi PJ, Adams DH: Chemokines and Chemokine Receptors as Therapeutic Targets in Inflammatory Bowel Disease; Pitfalls and Promise. J Crohns Colitis 2018, 12:S641-S52.
[20] Svensson M, Marsal J, Ericsson A, Carramolino L, Broden T, Marquez G, Agace WW: CCL25 mediates the localization of recently activated CD8alphabeta(+) lymphocytes to the small-intestinal mucosa. J Clin Invest 2002, 110:1113-21.
[21] Pietz G, De R, Hedberg M, Sjoberg V, Sandstrom O, Hernell O, Hammarstrom S, Hammarstrom ML: Immunopathology of childhood celiac disease-Key role of intestinal epithelial cells. PLoS One 2017, 12:e0185025.
[22] Atlasy N, Bujko A, Baekkevold ES, Brazda P, Janssen-Megens E, Lundin KEA, Jahnsen J, Jahnsen FL, Stunnenberg HG: Single cell transcriptomic analysis of the immune cell compartment in the human small intestine and in Celiac disease. Nat Commun 2022, 13:4920.
[23] Santos AJM, van Unen V, Lin Z, Chirieleison SM, Ha N, Batish A, Chan JE, Cedano J, Zhang ET, Mu Q, Guh-Siesel A, Tomaske M, Colburg D, Varma S, Choi SS, Christophersen A, Baghdasaryan A, Yost KE, Karlsson K, Ha A, Li J, Dai H, Sellers ZM, Chang HY, Dunn JCY, Zhang BM, Mellins ED, Sollid LM, Fernandez-Becker NQ, Davis MM, Kuo CJ: A human autoimmune organoid model reveals IL-7 function in coeliac disease. Nature 2024, 632:401-10.
[24] Barry M, Bleackley RC: Cytotoxic T lymphocytes: all roads lead to death. Nat Rev Immunol 2002, 2:401-9.
[25] Hay ZLZ, Slansky JA-O: Granzymes: The Molecular Executors of Immune-Mediated Cytotoxicity. LID - 10.3390/ijms23031833 [doi] LID - 1833.
[26] Rock KL, Reits E, Neefjes J: Present Yourself! By MHC Class I and MHC Class II Molecules. Trends Immunol 2016, 37:724-37.
[27] Breed ER, Lee ST, Hogquist KA: Directing T cell fate: How thymic antigen presenting cells coordinate thymocyte selection. Seminars in Cell & Developmental Biology 2018, 84:2-10.
[28] Han A, Newell EW, Glanville J, Fernandez-Becker N, Khosla C, Chien Y-h, Davis MM: Dietary gluten triggers concomitant activation of CD4+ and CD8+ αβ T cells and γδ T cells in celiac disease. Proceedings of the National Academy of Sciences 2013, 110:13073-8.
[29] Christophersen A, Zuhlke S, Lund EG, Snir O, Dahal-Koirala S, Risnes LF, Jahnsen J, Lundin KEA, Sollid LM: Pathogenic T Cells in Celiac Disease Change Phenotype on Gluten Challenge: Implications for T-Cell-Directed Therapies. Adv Sci (Weinh) 2021, 8:e2102778.

[30] Hogan MJ, Maheshwari N, Begg BE, Nicastri A, Hedgepeth EJ, Muramatsu H, Pardi N, Miller MA, Reilly SP, Brossay L, Lynch KW, Ternette N, Eisenlohr LC: Cryptic MHC-E epitope from influenza elicits a potent cytolytic T cell response. Nat Immunol 2023, 24:1933-46.
[31] Meresse B, Curran SA, Ciszewski C, Orbelyan G, Setty M, Bhagat G, Lee L, Tretiakova M, Semrad C, Kistner E, Winchester RJ, Braud V, Lanier LL, Geraghty DE, Green PH, Guandalini S, Jabri B: Reprogramming of CTLs into natural killer-like cells in celiac disease. Journal of Experimental Medicine 2006, 203:1343-55.
[32] Elmentaite R, Kumasaka N, Roberts K, Fleming A, Dann E, King HW, Kleshchevnikov V, Dabrowska M, Pritchard S, Bolt L, Vieira SF, Mamanova L, Huang N, Perrone F, Goh Kai'En I, Lisgo SN, Katan M, Leonard S, Oliver TRW, Hook CE, Nayak K, Campos LS, Dominguez Conde C, Stephenson E, Engelbert J, Botting RA, Polanski K, van Dongen S, Patel M, Morgan MD, Marioni JC, Bayraktar OA, Meyer KB, He X, Barker RA, Uhlig HH, Mahbubani KT, Saeb-Parsy K, Zilbauer M, Clatworthy MR, Haniffa M, James KR, Teichmann SA: Cells of the human intestinal tract mapped across space and time. Nature 2021, 597:250-5.
[33] Germain PL, Lun A, Garcia Meixide C, Macnair W, Robinson MD: Doublet identification in single-cell sequencing data using scDblFinder. F1000Res 2021, 10:979.
[34] Korsunsky I, Millard N, Fan J, Slowikowski K, Zhang F, Wei K, Baglaenko Y, Brenner M, Loh PR, Raychaudhuri S: Fast, sensitive and accurate integration of single-cell data with Harmony. Nat Methods 2019, 16:1289-96.
[35] Dominguez Conde C, Xu C, Jarvis LB, Rainbow DB, Wells SB, Gomes T, Howlett SK, Suchanek O, Polanski K, King HW, Mamanova L, Huang N, Szabo PA, Richardson L, Bolt L, Fasouli ES, Mahbubani KT, Prete M, Tuck L, Richoz N, Tuong ZK, Campos L, Mousa HS, Needham EJ, Pritchard S, Li T, Elmentaite R, Park J, Rahmani E, Chen D, Menon DK, Bayraktar OA, James LK, Meyer KB, Yosef N, Clatworthy MR, Sims PA, Farber DL, Saeb-Parsy K, Jones JL, Teichmann SA: Cross-tissue immune cell analysis reveals tissue-specific features in humans. Science 2022, 376:eabl5197.
[36] Ensari A, Marsh MN: Diagnosing celiac disease: A critical overview. Turk J Gastroenterol 2019, 30:389-97.
[37] Du Z, Lin JR, Rashid R, Maliga Z, Wang S, Aster JC, Izar B, Sorger PK, Santagata S: Qualifying antibodies for image-based immune profiling and multiplexed tissue imaging. Nat Protoc 2019, 14:2900-30.
[38] Wang F, Flanagan J, Su N, Wang LC, Bui S, Nielson A, Wu X, Vo HT, Ma XJ, Luo Y: RNAscope: a novel in situ RNA analysis platform for formalin-fixed, paraffin-embedded tissues. J Mol Diagn 2012, 14:22-9.
[39] Tsilingiri K, Barbosa T, Penna G, Caprioli F, Sonzogni A, Viale G, Rescigno M: Probiotic and postbiotic activity in health and disease: comparison on a novel polarised ex-vivo organ culture model. Gut 2012, 61:1007-15.
[40] Taavela J, Viiri K, Valimaki A, Sarin J, Salonoja K, Maki M, Isola J: Apolipoprotein A4 Defines the Villus-Crypt Border in Duodenal Specimens for Celiac Disease Morphometry. Front Immunol 2021, 12:713854.
[41] Ludvigsson JF, Bai JC, Biagi F, Card TR, Ciacci C, Ciclitira PJ, Green PH, Hadjivassiliou M, Holdoway A, van Heel DA, Kaukinen K, Leffler DA, Leonard JN, Lundin KE, McGough N, Davidson M, Murray JA, Swift GL, Walker MM, Zingone F, Sanders DS, Group BSGCDGD, British Society of

G: Diagnosis and management of adult coeliac disease: guidelines from the British Society of Gastroenterology. Gut 2014, 63:1210-28.
[42] Popp A, Taavela J, Graziano P, Parente P, Covelli C, Lamacchia C, Andriulli A, Maki M, Isola J: A New Intraepithelial gammadelta T-Lymphocyte Marker for Celiac Disease Classification in Formalin-Fixed Paraffin-Embedded (FFPE) Duodenal Biopsies. Dig Dis Sci 2021, 66:3352-8.
[43] Kirmizi A, Kalkan C, Yuksel S, Gencturk Z, Savas B, Soykan I, Cetinkaya H, Ensari A: Discriminant value of IEL counts and distribution pattern through the spectrum of gluten sensitivity: a simple diagnostic approach. Virchows Archiv 2018, 473:551-8.
[44] Hu X, Li J, Fu M, Zhao X, Wang W: The JAK/STAT signaling pathway: from bench to clinic. Signal Transduct Target Ther 2021, 6:402.
[45] Papadakis KA, Prehn J, Zhu D, Landers C, Gaiennie J, Fleshner PR, Targan SR: Expression and regulation of the chemokine receptor CXCR3 on lymphocytes from normal and inflammatory bowel disease mucosa. Inflamm Bowel Dis 2004, 10:778-88.
[46] Alam MS: Proximity Ligation Assay (PLA). Curr Protoc Immunol 2018, 123(1):e58.
[47] Bragde H, Jansson U, Jarlsfelt I, Soderman J: Gene expression profiling of duodenal biopsies discriminates celiac disease mucosa from normal mucosa. Pediatr Res 2011, 69:530-7.
[48] Olaussen RW, Johansen FE, Lundin KE, Jahnsen J, Brandtzaeg P, Farstad IN: Interferon-gamma-secreting T cells localize to the epithelium in coeliac disease. Scand J Immunol 2002, 56:652-64.
[49] Manes TD, Pober JS: Antigen presentation by human microvascular endothelial cells triggers ICAM-1-dependent transendothelial protrusion by, and fractalkine-dependent transendothelial migration of, effector memory CD4+ T cells. J Immunol 2008, 180:8386-92.
[50] Manes TD, Pober JS: Significant Differences in Antigen-Induced Transendothelial Migration of Human CD8 and CD4 T Effector Memory Cells. Arterioscler Thromb Vasc Biol 2016, 36:1910-8.
[51] Manes TD, Shiao SL, Dengler TJ, Pober JS: TCR signaling antagonizes rapid IP-10-mediated transendothelial migration of effector memory CD4+ T cells. J Immunol 2007, 178:3237-43.
[52] He WA-O, Gea-Mallorquí EA-OX, Colin-York HA-O, Fritzsche MA-O, Gillespie GA-OX, Brackenridge SA-O, Borrow PA-O, McMichael AA-O: Intracellular trafficking of HLA-E and its regulation. LID - 10.1084/jem.20221941 [doi] LID - e20221941.
[53] Hannoun Z, Lin Z, Brackenridge S, Kuse N, Akahoshi T, Borthwick N, McMichael A, Murakoshi H, Takiguchi M, Hanke T: Identification of novel HIV-1-derived HLA-E-binding peptides. Immunol Lett 2018, 202:65-72.
[54] Terrazzano G, Sica M, Gianfrani C, Mazzarella G, Maurano F, De Giulio B, de Saint-Mezard S, Zanzi D, Maiuri L, Londei M, Jabri B, Troncone R, Auricchio S, Zappacosta S, Carbone E: Gliadin regulates the NK-dendritic cell cross-talk by HLA-E surface stabilization. J Immunol 2007, 179:372-81.
[55] Kaufman J: Generalists and Specialists: A New View of How MHC Class I Molecules Fight Infectious Pathogens. Trends Immunol 2018, 39:367-79.
[56] Al-Lamki RS, Lu W, Manalo P, Wang J, Warren AY, Tolkovsky AM, Pober JS, Bradley JR: Tubular epithelial cells in renal clear cell carcinoma express high RIPK1/3 and show increased susceptibility to TNF receptor 1-induced necroptosis. Cell Death Dis 2016, 7.
[57] Gianfrani C, Troncone R, Mugione P, Cosentini E, De Pascale M, Faruolo C, Senger S, Terrazzano G, Southwood S, Auricchio S, Sette A: Celiac disease association with CD8+ T cell

responses: identification of a novel gliadin-derived HLA-A2-restricted epitope. J Immunol 2003, 170:2719-26.
[58] Picascia S, Sidney J, Camarca A, Mazzarella G, Giardullo N, Greco L, Auricchio R, Auricchio S, Troncone R, Sette A, Gianfrani C: Gliadin-Specific CD8(+) T Cell Responses Restricted by HLA Class I A*0101 and B*0801 Molecules in Celiac Disease Patients. J Immunol 2017, 198:1838-45.

Table 1. Percentage of PLA spots detected

Receptor: Ligand pairs	Control	Celiac	P value
TCRαβ/ HLA-E	1.54 ± 0.1%	10.25 ± 0.2%	****
TCRαβ/ HLA-B	1.22 ± 0.3%	9.98 ± 0.1%	****
TCRγδ/ HLA-E	1.12 ± 0.4%	5.22 ± 0.1%	****
TCRγδ/ HLA-B	1.09 ± 0.3%	8.35 ± 0.2%	****
NKG2C/HLA-E	0.27 ± 0.1%	3.29 ± 0.1%	****
TCRαβ/ HLA-DR	1.52 ± 0.1%	2.25 ± 0.6%	ns

Table shows the average percentage of in-situ PLA spot detected protein complexes between αβ and γδ T cells and ligands HLA-E, HLA-B, or HLA-DR. NKG2C receptor binding to HLA-E was also determined. Binding was assessed on T cells in the villous epithelium in control and celiac biopsies. Data presented (PLA signal per high power field) are means ± S.E.M., n = 6 individual biopsies each with ten images. ***$p < 0.0001$ by Mann-Whitney test.

Figure Legends

Figure 1. Single cell RNAseq analysis of CeD and control biopsies

Left: UMAP embedding and cluster annotation of duodenal cells from biopsies isolated from patients with CeD(celiac) or healthy controls (control). Right: Distribution of clusters within from celiac vs control groups in the same UMAP embedding. Two celiac biopsies and two control biopsies were analyzed using the 10x genomics single cell RNA sequencing platform. **(A)** UMAP embedding of T and NK cell clusters **(B).** UMAP embedding showing distribution of cells from celiac vs control groups **(C).** Proportions of T cells and NK cells in celiac vs control groups **(D).** IFNG expression shown in UMAP embedding of total T and NK cell clusters **(E).** IFNG expression in activated CD8+ T cells in celiac vs control groups **(F)** IFNGR1 expression in enterocytes in celiac vs control groups **(G).** IFNGR1 expression in villous enterocytes marked by APOA4 expression in celiac vs control groups **(H)**

Figure 2. Quantitation of total CD3, TCR αβ and TCR γδ T cells within the duodenal villous and crypt epithelium in CeD vs. control biopsies.

Representative tiled biopsies were taken from CeD and control specimens to assess tissue morphology using pan-epithelial cell marker E-cadherin (**A**). Different regions of the epithelium were identified in magnified images using a marker for villous enterocytes ApoA4 and for transitional zone crypt enterocytes Ki-67 to determine the villous/crypt border. The dotted white lines follow the basement membrane that separates villous and crypt epithelium from the lamina propria. **(B).** Representative images of CD3 (red) infiltration in the villous (**C**) or crypt (**G**) in celiac vs controls samples. Cells are also labeled with either TCRαβ or γδ (green).

Quantitiation of the frequencies of total CD3 T cells (N=9) (**D, H)** TCR $\alpha\beta$ **(**N=7) **(E, I)** and $\gamma\delta$ T cells (N = 7) (**F, J)** cells in the villous and crypt epithelium are presented as the ratio of T cells per enterocyte nuclei (stained with DAPI). Each point represents one biopsy and the bars represent mean ± SEM. Significance was determined by t-test. *P ≤ 0.05; **P ≤ 0.01; ***P ≤ 0.001.

Figure 3. Identification of intraepithelial CD3 T cells in CeD as activated CTL.

Granzyme B protein expression was assessed by IF staining as the percentage of CD3 cells positive for Granzyme B within the villous epithelium of CeD vs control biopsies (N = 9) **(A, B)**. Ki-67 (N=12) **(C, D)**, NKG2C (N= 8) and DAP12 (N = 8) **(E, F)** protein expression were also assessed by IF as the percentage of CD3 cells that were positive within the villous of biopsies. Expression values of MKI67, KLRC2 and TYROBP(DAP12) in T cells from scRNA seq experiments **(G).** Each dot represents one biopsy and the bars represent mean ± SEM. Significance determined by t-test. *P ≤ 0.05; **P ≤ 0.01; ***P ≤ 0.001.

Figure 4. Evidence that villous enterocytes in CeD but not controls display IFNγ-mediated signaling.

CeD and control biopsies were labeled with pSTAT1 antibody. Images show pSTAT1 (green) expression in control and CeD biopsies **(A).** The percentage of villous or crypt nuclei positive for pSTAT1 was calculated (N = 15) (**B)**. Representative images of HLA-DR (green) expression in control and CeD biopsies **(C).** HLA-DR expression by enterocytes in CeD and control biopsies was determined by calculating the percent area of HLA-DR expression normalized to epithelial area (N = 11) **(D).** Expression values of HLA Class II genes in enterocytes from celiac vs control

groups **(E).** Each dot represents one biopsy and the bars represent mean ± SEM. t-test. *$P \leq 0.05$; **$P \leq 0.01$; ***$P \leq 0.001$.

Figure 5. Chemokine transcript and receptor expression in CeD and control biopsies. Control and celiac biopsies were stained with CD3 (red) and chemokine receptors (green) CXCR3 **(A),** CCR5 **(C),** and CCR9 **(E).** Expression of each chemokine receptor was determined by calculating the mean fluorescent intensity (MFI) of CXCR3 (N = 9) (**B)**, CCR5 (N = 8) **(D)**, and CCR9 (N = 9) **(F)** among all CD3 cells in the villous. RNAscope was used to determine expression of chemokines CCL3, CCL4 **(G, H);** CXCL10, CXCL11 **(J, K);** and CCL25 **(L).** by calculating the average number of transcripts in the villous epithelium of CeD and control biopsies per field at 40X. Immunofluorescent images show transcript expression of chemokines (green) with epithelium labeled using EPCAM (white) and T cells with CD3 (red) in the villous of biopsies. Tissues were counterstained with Hoechst for nuclei (N=6). CCL5 transcript expression in IFNG+ and IFNG- cells (**K).** Each dot for IF represents one biopsy and the bars represent mean ± SEM. t-test. *$P \leq 0.05$; **$P \leq 0.01$; ***$P \leq 0.001$.

Figure 6. Assessment of HLA-I expression on villous enterocytes in CeD and controls. Representative images show immunofluorescent expression of each MHC-I molecule (green) HLA-B **(A**), HLA-E (**C**), and β2-microglobulin (**C)** in the villous epithelium of biopsies. Surface expression of HLA-B (N=12) **(A)**, HLA-E (N=12) **(C)**, and β2-microglobulin (N=11) **(D)** on CeD and control biopsies was calculated using the mean fluorescent intensity of each ligand and

normalizing to the villous area. Each dot represents one biopsy and the bars represent mean ± SEM. t-test. *$P \leq 0.05$; **$P \leq 0.01$; ***$P \leq 0.001$.

Figure 7. Quantification interacts between TCRs and NKG2C on intraepithelial CTL with enterocyte class I HLA molecules.

Proximity ligation assays were used to estimate the frequency of binding between TCR$\alpha\beta$, TCR$\gamma\delta$, and NKG2C to different MHC-I ligands in the villous epithelium. Biopsies were co-labeled with CD3 (green), Collagen IV (white), and counterstained with Hoechst (blue) to identity intraepithelial T cells. Data represent the percentage of CD3 cells with PLA spots per multiple 40x fields. Graphs quantify close interactions of TCR $\alpha\beta$ to HLA-E (N = 6) (**A, B)** or HLA-B (N = 6) **(C, D)**, TCR $\gamma\delta$ to HLA-E (N = 6) **(E, F)** or HLA-B (N=6) **(G, H)**, and NKG2C to HLA-E (N=6) (**I, J).** Binding of TCR $\alpha\beta$ or $\gamma\delta$ with HLA-DR was also assessed as a control (**K-N**). Each dot represents one field and the bars represent mean ± SEM. t-test. *$P \leq 0.05$; **$P \leq 0.01$; ***$P \leq 0.001$.

Figure 1

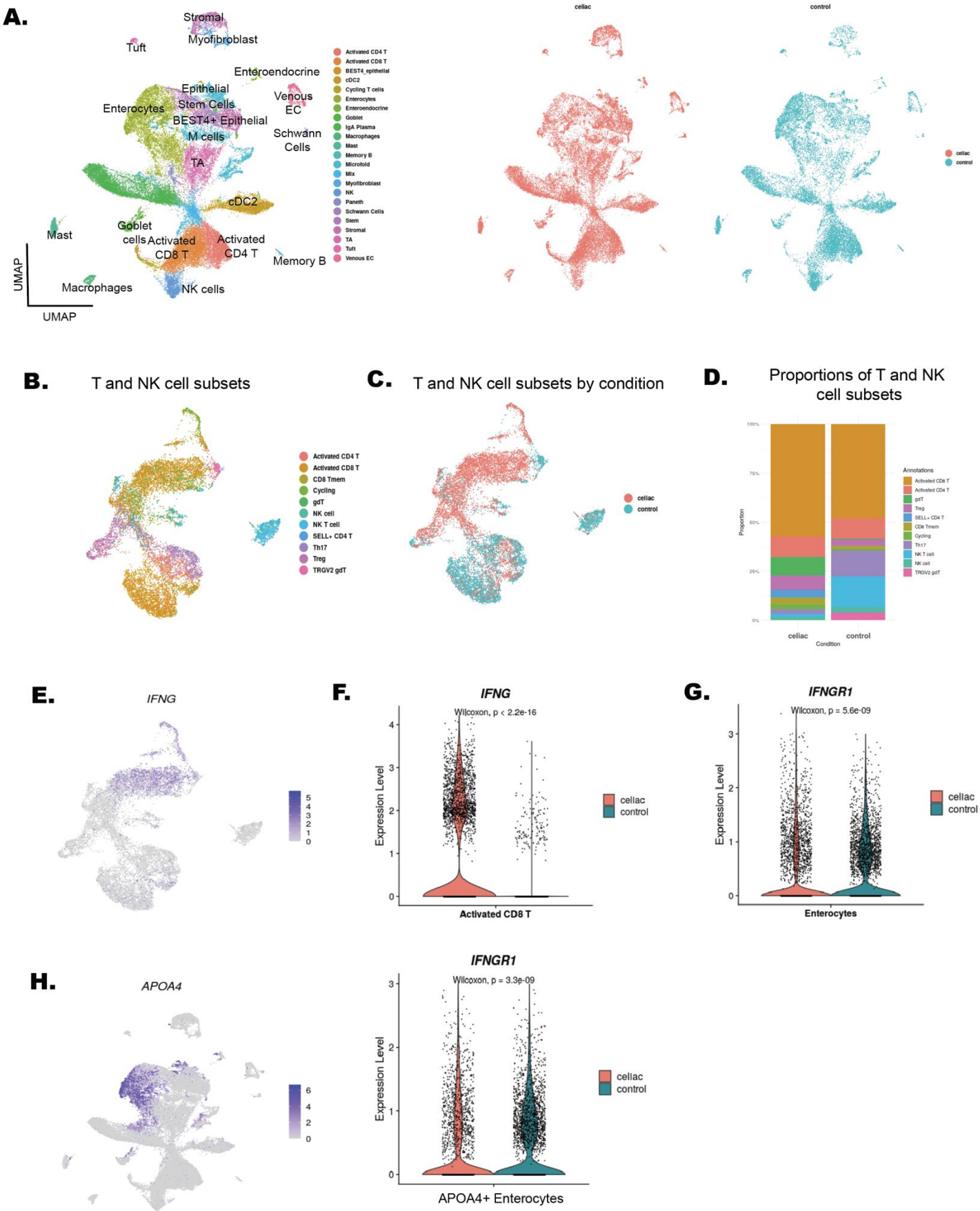
A.
Stromal
Myofibroblast
Tuft
Enteroendocrine
Epithelial
Stem Cells
Enterocytes
BEST4+ Epithelial
M cells
Venous EC
Schwann Cells
TA
cDC2
Mast
Goblet cells
Activated CD8 T
Activated CD4 T
Memory B
Macrophages
NK cells
UMAP
UMAP
Activated CD4 T
Activated CD8 T
BEST4_epithelial
cDC2
Cycling T cells
Enterocytes
Enteroendocrine
Goblet
IgA Plasma
Macrophages
Mast
Memory B
Microfold
Mix
Myofibroblast
NK
Paneth
Schwann Cells
Stem
Stromal
TA
Tuft
Venous EC
celiac
control
celiac
control
B.
T and NK cell subsets
Activated CD4 T
Activated CD8 T
CD8 Tmem
Cycling
gdT
NK cell
NK T cell
SELL+ CD4 T
Th17
Treg
TRGV2 gdT
C.
T and NK cell subsets by condition
celiac
control
D.
Proportions of T and NK cell subsets
100%
75%
50%
25%
0%
Proportion
celiac
control
Condition
Annotations
Activated CD8 T
Activated CD4 T
gdT
Treg
SELL+ CD4 T
CD8 Tmem
Cycling
Th17
NK T cell
NK cell
TRGV2 gdT
E.
IFNG
5
4
3
2
1
0
F.
IFNG
Wilcoxon, p < 2.2e-16
Expression Level
4
3
2
1
0
Activated CD8 T
celiac
control
G.
IFNGR1
Wilcoxon, p = 5.6e-09
Expression Level
3
2
1
0
Enterocytes
celiac
control
H.
APOA4
6
4
2
0
IFNGR1
Wilcoxon, p = 3.3e-09
Expression Level
3
2
1
0
APOA4+ Enterocytes
celiac
control

Figure 2

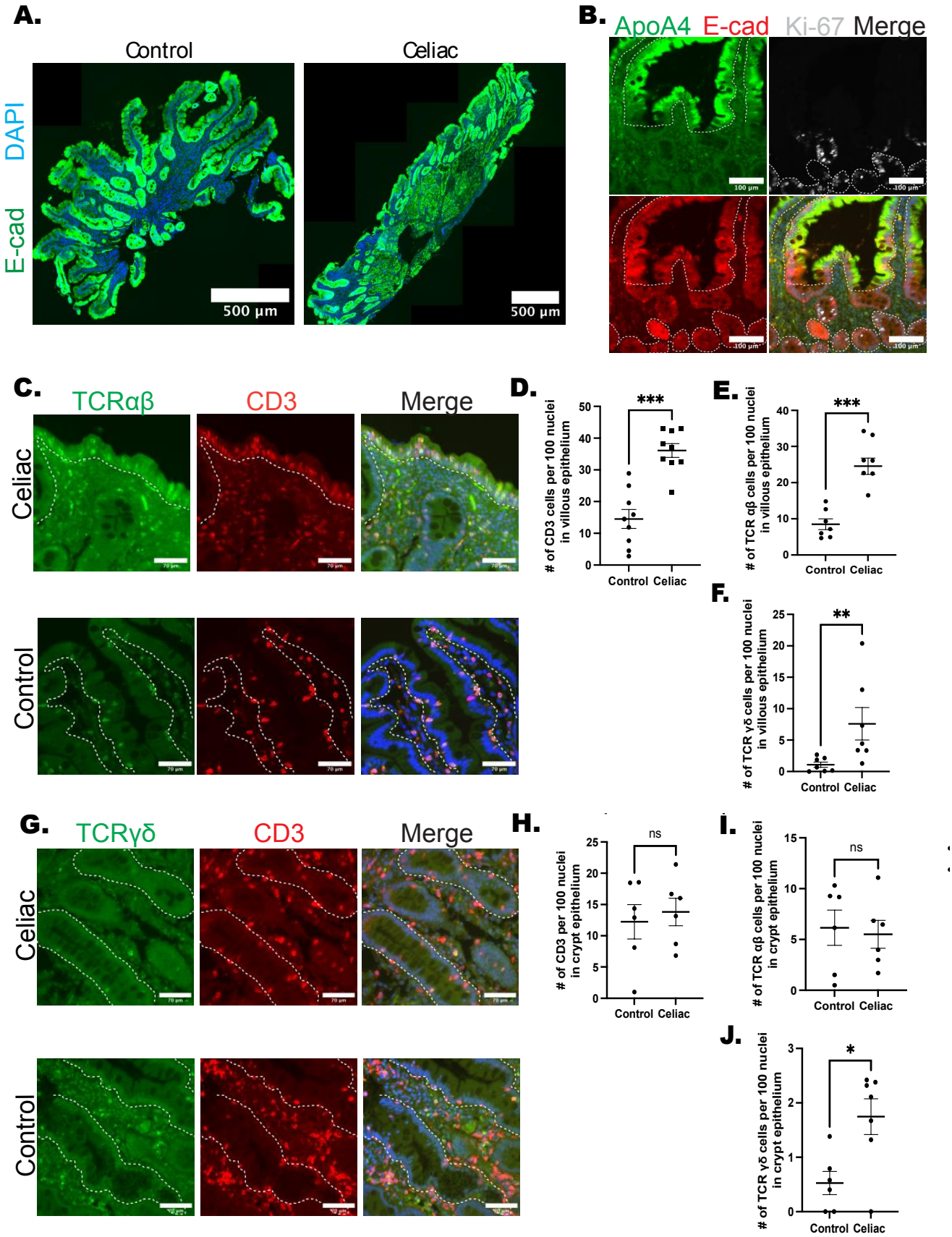
A.
Control
Celiac
DAPI
E-cad
500 µm
500 µm
B.
ApoA4
E-cad
Ki-67
Merge
100 µm
C.
TCRαβ
CD3
Merge
Celiac
Control
D.
# of CD3 cells per 100 nuclei in villous epithelium
***
Control
Celiac
E.
# of TCR αβ cells per 100 nuclei in villous epithelium
***
F.
# of TCR γδ cells per 100 nuclei in villous epithelium
**
G.
TCRγδ
CD3
Merge
H.
# of CD3 per 100 nuclei in crypt epithelium
ns
I.
# of TCR αβ cells per 100 nuclei in crypt epithelium
ns
J.
# of TCR γδ cells per 100 nuclei in crypt epithelium
*

Figure 3

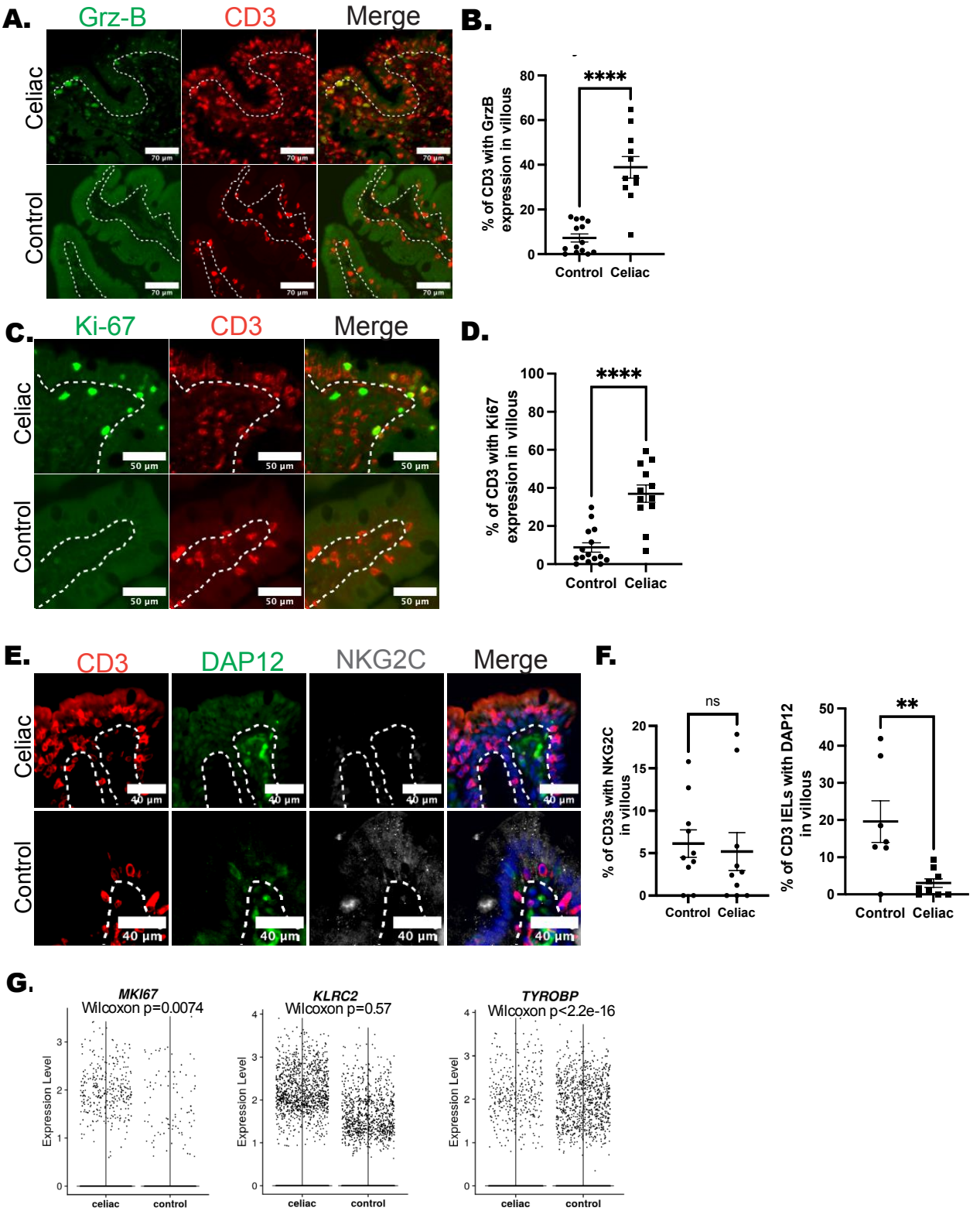
A.
Grz-B
CD3
Merge
Celiac
Control
70 µm
B.
% of CD3 with GrzB expression in villous
****
Control
Celiac
C.
Ki-67
CD3
Merge
Celiac
Control
50 µm
D.
% of CD3 with Ki67 expression in villous
****
Control
Celiac
E.
CD3
DAP12
NKG2C
Merge
Celiac
Control
40 µm
F.
% of CD3s with NKG2C in villous
ns
Control
Celiac
% of CD3 IELs with DAP12 in villous
**
Control
Celiac
G.
MKI67
Wilcoxon p=0.0074
KLRC2
Wilcoxon p=0.57
TYROBP
Wilcoxon p<2.2e-16
Expression Level
celiac
control

Figure 4

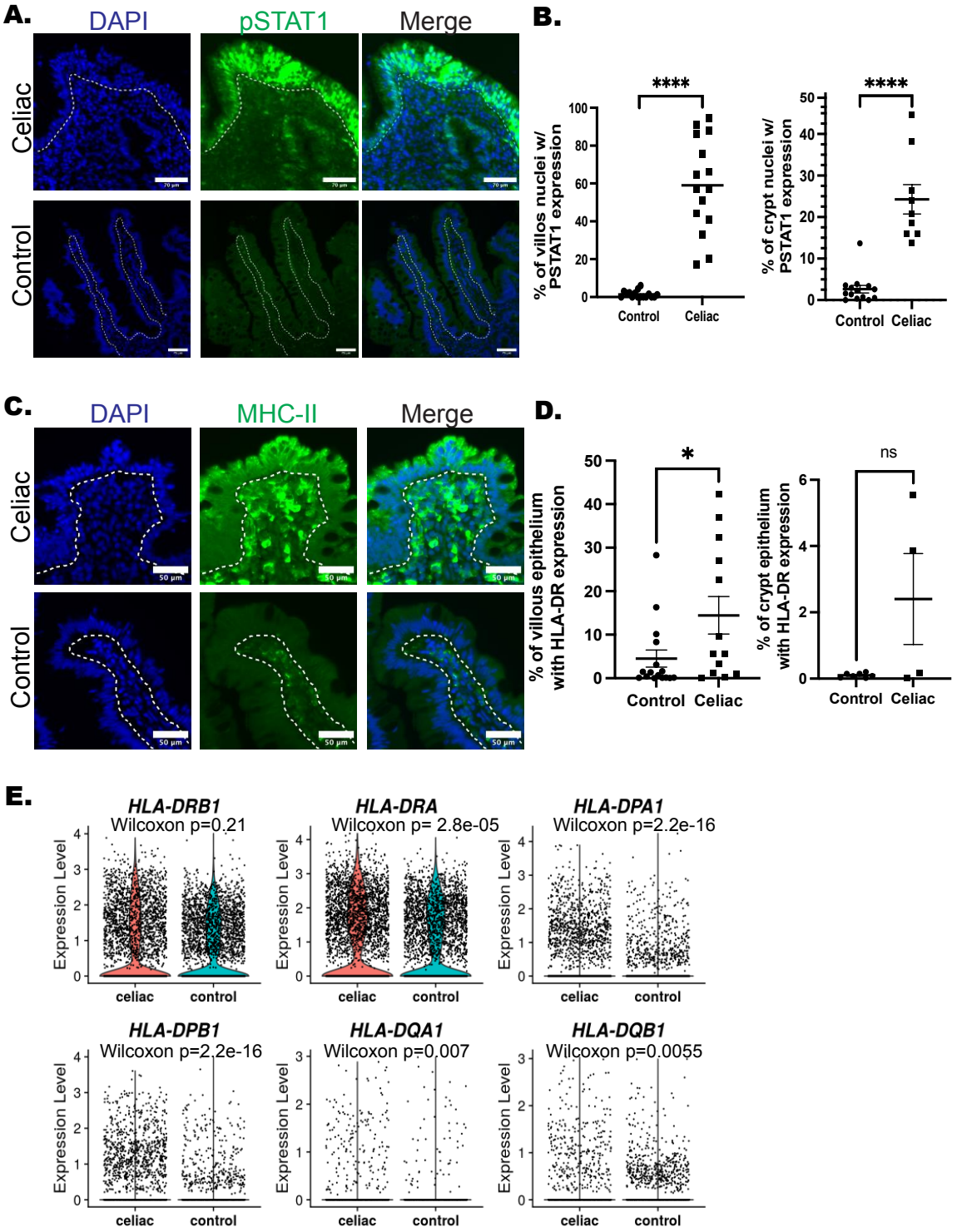
A.
DAPI
pSTAT1
Merge
Celiac
Control
B.
****
% of villos nuclei w/ PSTAT1 expression
Control
Celiac
****
% of crypt nuclei w/ PSTAT1 expression
Control
Celiac
C.
DAPI
MHC-II
Merge
Celiac
Control
D.
*
% of villous epithelium with HLA-DR expression
Control
Celiac
ns
% of crypt epithelium with HLA-DR expression
Control
Celiac
E.
HLA-DRB1
Wilcoxon p=0.21
HLA-DRA
Wilcoxon p= 2.8e-05
HLA-DPA1
Wilcoxon p=2.2e-16
HLA-DPB1
Wilcoxon p=2.2e-16
HLA-DQA1
Wilcoxon p=0.007
HLA-DQB1
Wilcoxon p=0.0055
Expression Level
celiac
control

Figure 5

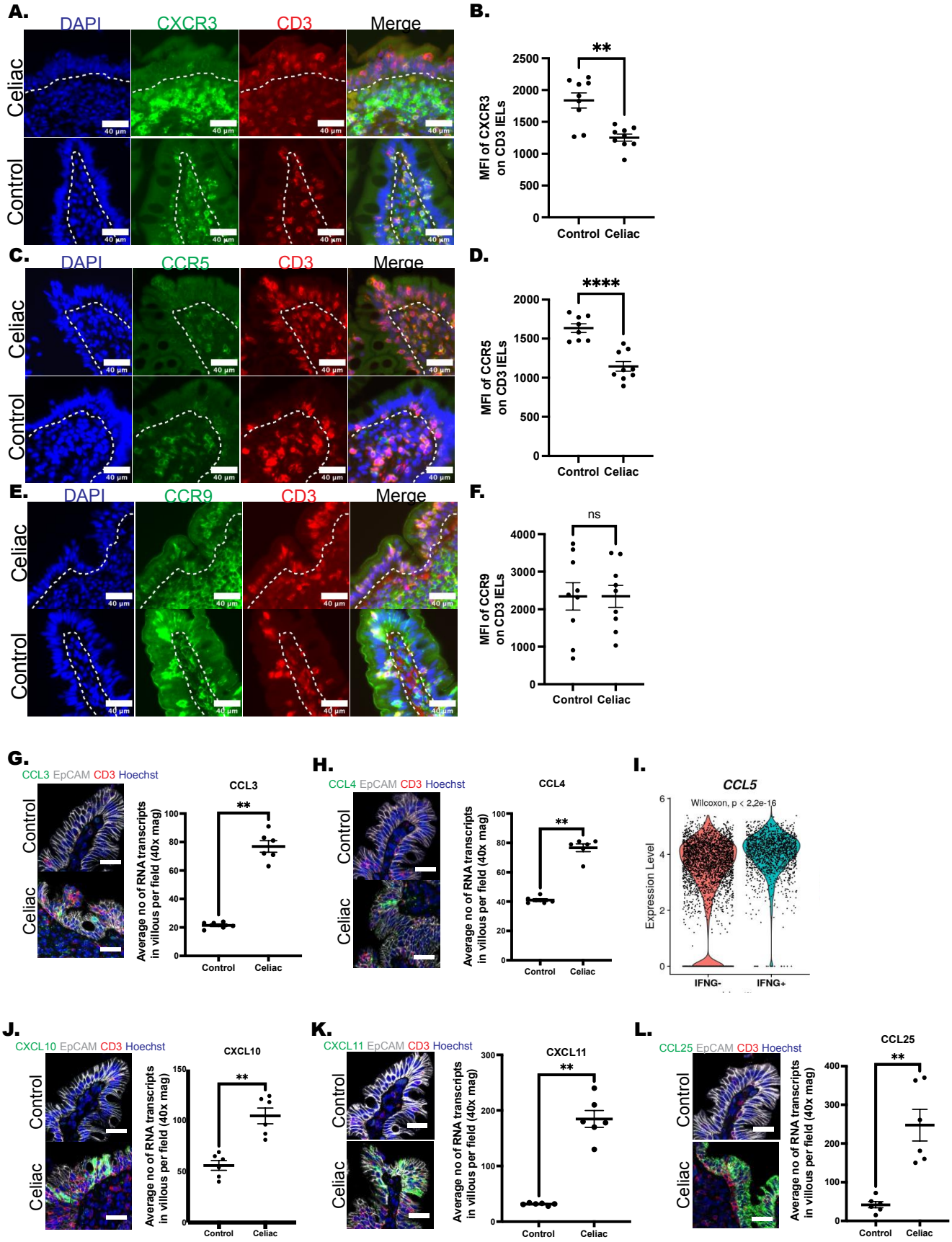
A.
DAPI
CXCR3
CD3
Merge
Celiac
Control
40 µm
B.
MFI of CXCR3 on CD3 IELs
**
Control
Celiac
C.
DAPI
CCR5
CD3
Merge
D.
MFI of CCR5 on CD3 IELs
****
E.
DAPI
CCR9
CD3
Merge
F.
MFI of CCR9 on CD3 IELs
ns
G.
CCL3 EpCAM CD3 Hoechst
CCL3
Average no of RNA transcripts in villous per field (40x mag)
H.
CCL4 EpCAM CD3 Hoechst
CCL4
I.
CCL5
Wilcoxon, p < 2.2e-16
Expression Level
IFNG-
IFNG+
J.
CXCL10 EpCAM CD3 Hoechst
CXCL10
K.
CXCL11 EpCAM CD3 Hoechst
CXCL11
L.
CCL25 EpCAM CD3 Hoechst
CCL25

Fig 6

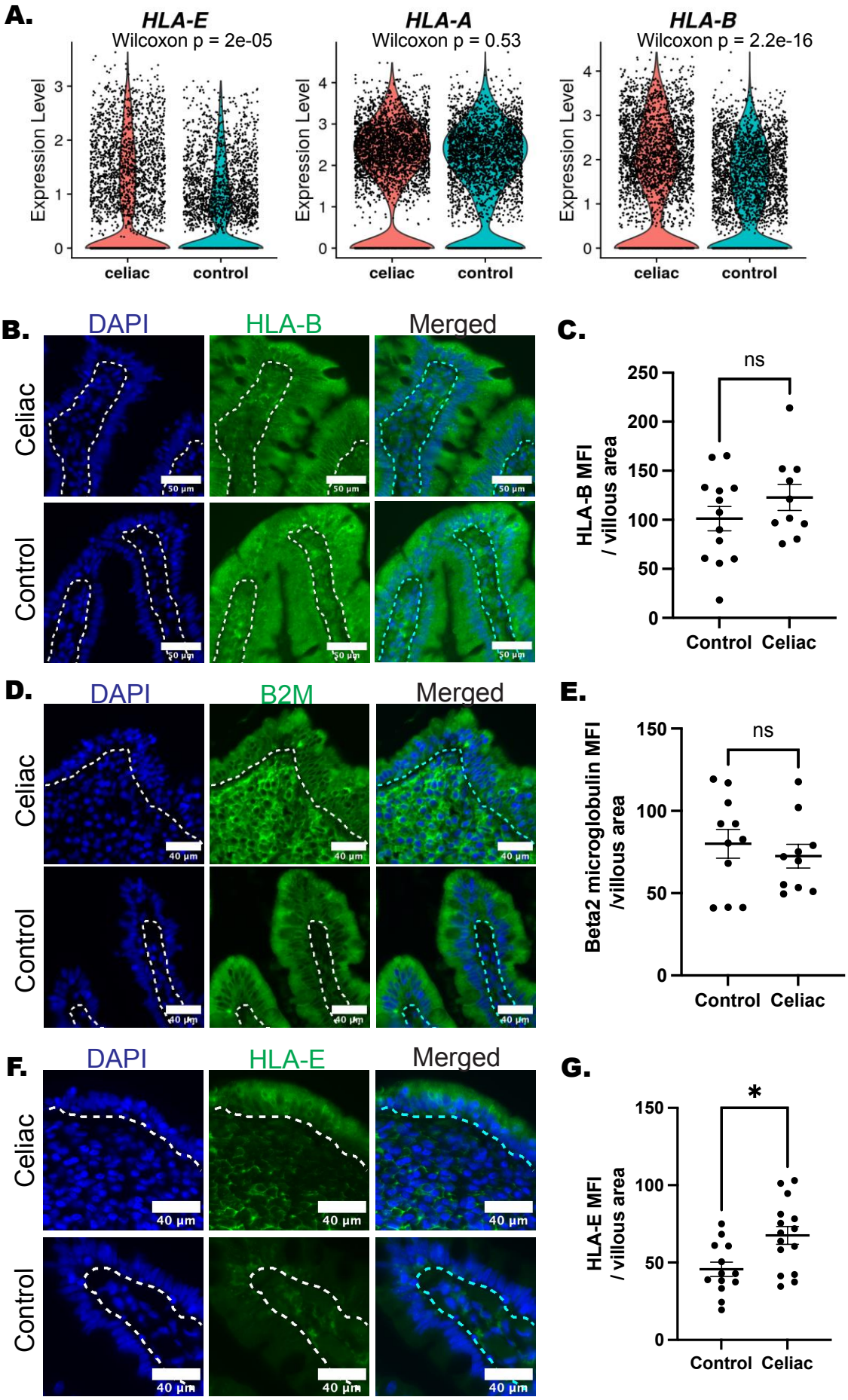
A.
HLA-E
Wilcoxon p = 2e-05
HLA-A
Wilcoxon p = 0.53
HLA-B
Wilcoxon p = 2.2e-16
Expression Level
celiac
control
B.
DAPI
HLA-B
Merged
Celiac
Control
50 µm
C.
ns
HLA-B MFI / villous area
Control
Celiac
D.
DAPI
B2M
Merged
Celiac
Control
40 µm
E.
ns
Beta2 microglobulin MFI /villous area
Control
Celiac
F.
DAPI
HLA-E
Merged
Celiac
Control
40 µm
G.
*
HLA-E MFI / villous area
Control
Celiac

Figure 7

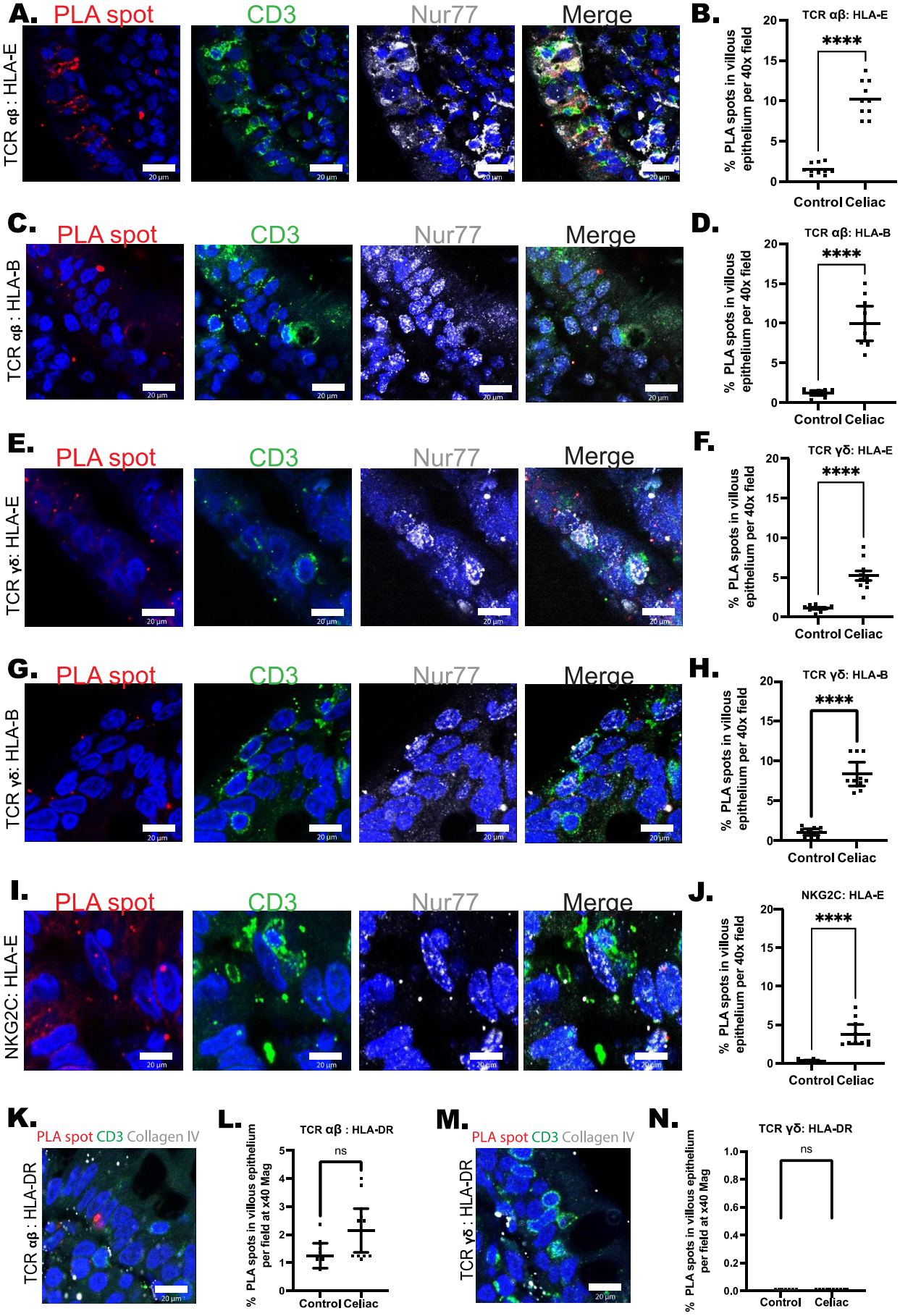
A.
PLA spot
CD3
Nur77
Merge
TCR αβ : HLA-E
20 µm
B.
TCR αβ: HLA-E
****
% PLA spots in villous epithelium per 40x field
Control Celiac
C.
TCR αβ : HLA-B
D.
TCR αβ: HLA-B
E.
TCR γδ: HLA-E
F.
TCR γδ: HLA-E
G.
TCR γδ: HLA-B
H.
TCR γδ: HLA-B
I.
NKG2C: HLA-E
J.
NKG2C: HLA-E
K.
PLA spot CD3 Collagen IV
TCR αβ : HLA-DR
L.
TCR αβ : HLA-DR
ns
% PLA spots in villous epithelium per field at x40 Mag
M.
TCR γδ : HLA-DR
N.
TCR γδ: HLA-DR
Control
Celiac